Technical Report ECOM-0138-5 May 1969

COAXIAL MICROWAVE BANDPASS FILTERS

C.E.L. Technical TM Memorandum No. 100

Contract No. DAAB 07-68-C-0138
DA Project No. 1 HO 21101 A04 01 02

Prepared by

W. Alan Davis

COOLEY ELECTRONICS LABORATORY

Department of Electrical Engineering
The University of Michigan
Ann Arbor, Michigan

for

U.S. Army Electronics Command, Fort Monmouth, N.J.

engm

UMRØ611

ABSTRACT

A review of lumped element filter synthesis techniques using the power loss ratio is presented. This leads to filter synthesis based on impedance inverters for which S. B. Cohn (Ref. 1) has given an approximate microwave realization. Here an improved method is presented which considers the distributive property of the impedance inverter. Several theoretical curves are shown comparing the two methods. Finally results from an experimental model are shown.

FOREWORD

This study on microwave bandpass filters was motivated by the need for a filter that could be constructed completely within a coaxial line. There is no single source in the literature which describes the principles and derives the relations used here. Also there is little information on how these principles may be applied to coaxial bandpass filters.

However, after applying these principles to a coaxial filter, some empirical modification is required because the design is based on approximating a lumped-reactive element with a distributed element. Therefore, this theory was improved by accounting for the nonzero length of the reactive element. These new design formulas give a filter characteristic which resembles the desired characteristic to a much greater degree than the older method.

The purpose of this study is to bring together the principles and derivations needed for the construction of a microwave bandpass filter. With this information and appropriate tables for a low-pass prototype circuit an engineer can design a coaxial microwave bandpass filter for a desired bandwidth and for Chebyshev filters a desired passband ripple. The theory developed there applies equally well to bandpass impedance matching networks. In addition to the information mentioned above, the designer needs to know only the Q of the load and the load impedance level.

The formulas are simple to use and sufficiently exact so that no additional empirical modification is needed. The filter is easy to make since it consists only of a coaxial line and some disks. Both of the above considerations are important in reducing fabrication costs.

TABLE OF CONTENTS

LIST OF ILLUSTRATIONS

LIST OF ILLUSTRATIONS (Cont.)

LIST OF ILLUSTRATIONS (Cont.)

LIST OF TABLES

COAXIAL MICROWAVE BANDPASS FILTERS

I. General Discussion

At low frequencies a very general and complete filter synthesis technique has been developed which utilizes lumped inductors and capacitors as the basic building blocks. At microwave frequencies distributed parameter elements are used which makes filter synthesis more complicated. Since these elements have a complex frequency dependence, no complete filter synthesis technique has been developed. However, lumped techniques have been an invaluable guide to microwave filter synthesis.

The following discussion presents the necessary equations and outlines a procedure for designing bandpass impedance matching networks in coaxial transmission lines. The method of analysis starts by defining the desired frequency dependence of the reflection coefficient of the network. A low-pass lumped-prototype circuit is developed which is transformed into a bandpass circuit. The use of impedance inverters (a device which takes the reciprocal of the impedance) is found necessary to realize the lumped prototype in a distributed circuit. An impedance inverter is realized by a disk and a small length of line. Since a coaxial disk introduces discontinuity capacitance, the design is modified to take this into account. Finally, an example is given to show how these relations are used. In short, a review of filter synthesis is presented which is followed by an improved synthesis technique for the impedance inverter.

II. Power Loss Ratio

The power loss ratio or transducer loss ratio is defined as the incident or available power divided by the power delivered to the load (Ref. 2, pp. 403-410).

$$P_{LR} = \frac{|V_g|^2 R_L}{4R_g |V_L|^2} = \frac{1}{1 - \Gamma\Gamma^*} = \frac{1}{1 - \rho^2} \tag{1}$$

The symbol Γ is the input reflection coefficient of a lossless network terminated by a resistive load R_L. This synthesis method begins by choosing the reflection coefficient of the network which for passive circuits is restricted to the range $0 \leq \Gamma(\omega) \leq 1$. For a transmission line with characteristic impedance Z_o terminated with an impedance $Z_L = R + jX$ the reflection coefficient is

$$\Gamma(\omega) = \frac{Z_L - Z_o}{Z_L + Z_o} = \frac{R(\omega) - Z_o + jX(\omega)}{R(\omega) + Z_o + jX(\omega)} \tag{2}$$

If m and n denote the even and odd parts of the polynomials respectively, the load impedance is (Ref. 3, p. 22)

$$Z_L = \frac{m_1 + n_1}{m_2 + n_2} \tag{3}$$

When s, the complex frequency, is $j\omega$, Eq. 4 below shows that the even parts are real and the odd parts are imaginary.

$$Z_L = \frac{(m_1 + n_1)(m_2 - n_2)}{(m_2 + n_2)(m_2 - n_2)}$$

$$Z_L = \frac{m_1 m_2 - n_1 n_2}{m_2^2 - n_2^2} + \frac{m_2 n_1 - m_1 n_2}{m_2^2 - n_2^2} = R(\omega) + jX(\omega) \tag{4}$$

Therefore $R(\omega)$ is an even function and $X(\omega)$ is an odd function of ω. This property is used in Eq. 2 to show

$$\Gamma(-\omega) = \frac{R(\omega) - Z_o - jX(\omega)}{R(\omega) + Z_o - jX(\omega)} = \Gamma^*(\omega) \tag{5}$$

Since $\Gamma(\omega)\Gamma(-\omega) = \rho^2$, it is apparent that ρ^2 is an even function of ω. The power loss ratio is the ratio of even polynomials which from Eq. 1 can be expressed as

$$P_{LR} = 1 + \frac{(R - Z_o)^2 + X^2}{4RZ_o} \triangleq 1 + \frac{P(\omega^2)}{Q^2(\omega)} \tag{6}$$

For the case of a low-pass Chebyshev filter, this last ratio is chosen as

$$P_{LR} = 1 + k^2 T_n^2(\omega/\omega_c) \tag{7}$$

where ω_c is the cutoff frequency, k^2 is the passband tolerance, and T_n is the Chebyshev polynomial of degree n.

$$T_n(\omega/\omega_c) = \cos\left[n \operatorname{Arccos}(\omega/\omega_c)\right] \tag{8}$$

T_n oscillates between ± 1 for $|\omega/\omega_c| \leq 1$ and equals one when $|\omega/\omega_c| = 1$.

III. Lumped Low-Pass Prototype Circuit

A low-pass filter may be realized by either of two dual prototype lumped ladder networks as shown in Figs. 1 and 2.

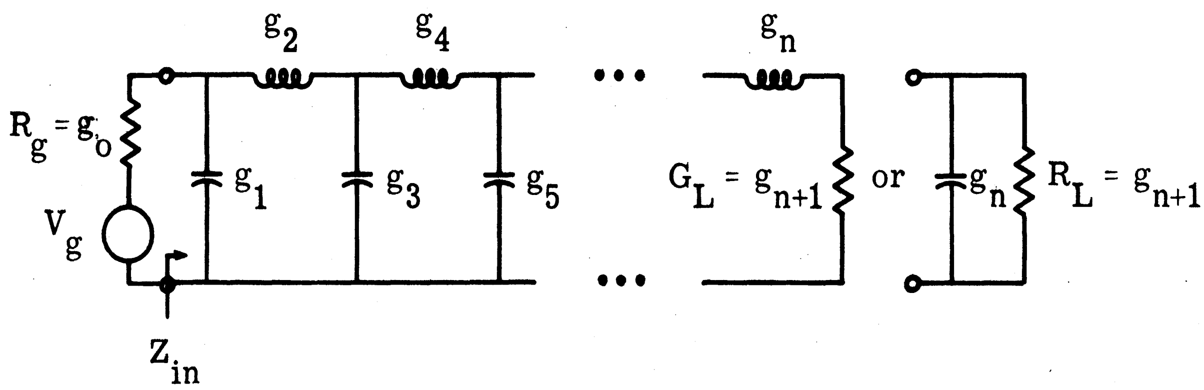

Fig. 1. Low-pass prototype circuit starting with shunt capacitor

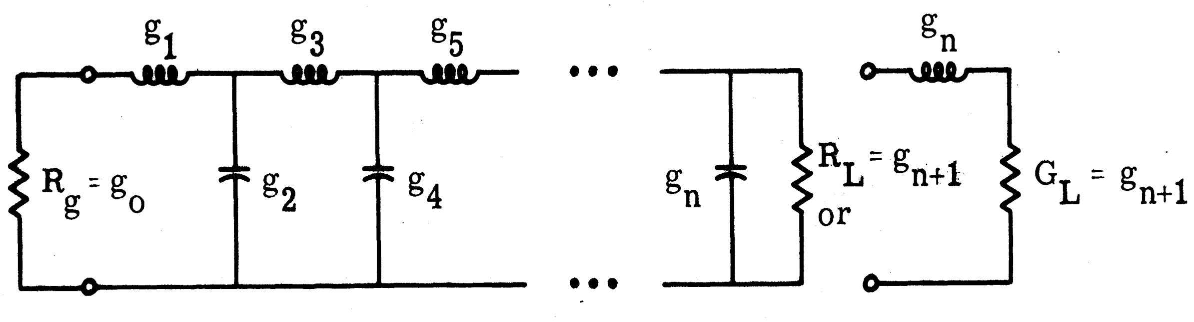

Fig. 2. Low-pass prototype circuit starting with series inductor

A relationship must be found between these two lumped circuits and the power loss ratio which was defined in terms of a transmission line. In particular a transmission and reflection coefficient will be found for the more general network of Fig. 3 where the source and load are connected by an arbitrary lossless network with $Z_1 = V_1/I_1 = R_{11} + jX_{11}$.

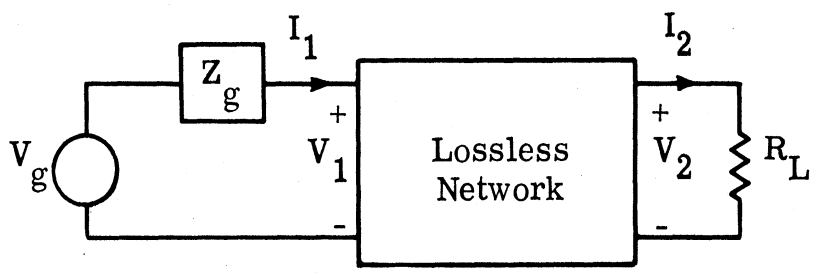

Fig. 3. Lossless network fed through an arbitrary generator impedance

Since the network is lossless, the average power entering port 1 must equal the average power leaving at port 2.

$$\frac{|V_g|^2 R_{11}}{|Z_g + Z_1|^2} = \frac{|V_2|^2}{R_L} \tag{9}$$

This expression may be rearranged to give the ratio of power delivered to the load to the available power from the generator.

$$\frac{|V_2|^2 4R_g}{R_L |V_g|^2} = \frac{4R_{11} R_g}{|Z_g + Z_1|^2} \tag{10}$$

This is seen to be equivalent to the transmission coefficient as the term on the right-hand side is

$$1 - \left|\frac{Z_1 - Z_g^*}{Z_1 + Z_g}\right|^2 = 1 - \frac{(R_{11} - R_g)^2 + (X_g + X_{11})^2}{|Z_g + Z_1|^2} = \frac{4R_g R_{11}}{|Z_g + Z_1|^2}$$

Therefore the reciprocal power loss ratio or transmission coefficient for the circuit of Fig. 3 is simply

$$|t|^2 = \frac{V_2^2 / R_L}{V_g^2 / (4R_g)} = 1 - \left| \frac{Z_1 - Z_g^*}{Z_1 + Z_g} \right|^2 = 1 - |\Gamma|^2 \tag{11}$$

Thus the reflection coefficient of the low-pass prototype circuit of Fig. 1 is

$$\Gamma = \frac{Z_{in} - R_g}{Z_{in} + R_g} \tag{12}$$

where Z_{in} is the input impedance of the ladder network as seen from the terminals of the generator resistance. To derive the particular g values for the circuit of Fig. 1, the two expressions for the power loss ratio are equated.

$$P_{LR} = 1 + k^2 T_n^2 (\omega/\omega_c) = \frac{1}{1 - |\Gamma|^2} \tag{13}$$

The left hand side defines the ripple factor k, the cutoff frequency ω_c, and the number of elements n. The right hand side is a function of the lumped prototype circuit g values which can now be found. Explicit expressions exist for the g_k for both the maximally flat and the Chebyshev filters. However, tabulated values will be used subsequently and they may be found in various references (i.e., Ref. 4). A similar procedure is used for the case of the filter of Fig. 2.

IV. Impedance Matching with Lumped Low-Pass Networks[1]

A low-pass Chebyshev impedance matching network is shown in Fig. 4.

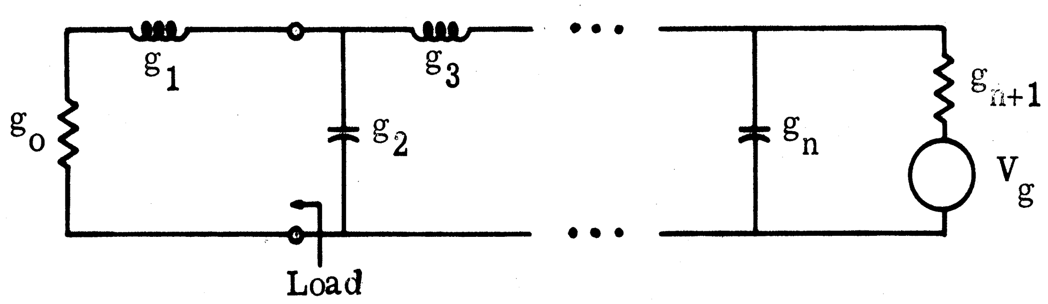

Fig. 4. Low-pass matching network

This network can be designed either to provide minimum reflection or to provide a specified ripple in the passband. The first criteria is the one used in the example later. The load is considered to consist of both g_o and g_1. An optimum impedance matching network must necessarily have a filter-like characteristic. Also, if the load has a reactive part, it is impossible to have perfect power transmission over a range of frequencies. Overall power transmission may be improved, however, if a small amount of power is reflected at all frequencies in the passband.

The load is characterized by the decrement

$$\delta \triangleq \frac{1}{g_1 g_o \omega_c'} \tag{14}$$

where ω_c' is the cutoff frequency for the low-pass circuit of Fig. 4. The published tables and curves for the g_k $(k = 1, 2, \ldots, n)$ are normalized to $\omega_c' = 1$. Hence these g_k values must be remultiplied by ω_c' when used. The decrement can be written in terms of the resonated Q_A of

[1] Ref. 4, p. 120.

the load, which by use of a reactive element has been tuned to resonate at ω_o, and the fractional bandwidth w.

$$\delta = \frac{1}{wQ_A} \tag{15}$$

This definition will be convenient for bandpass matching structures described later, and it emphasizes that the decrement is the reciprocal Q of the load at the edge of the impedance matching band. Better matching and lower ripple can be achieved by using more filter elements although beyond $n = 3$ or 4, there is only slight improvement. The calculation of the g values for the impedance matching network of Fig. 4 is complicated so curves found in Ref. 4 (pp. 126-129) are used to get the element values.

V. Bandpass Matching Networks

At microwave frequencies bandpass rather than low-pass impedance matching networks are usually desired. For the bandpass case both the load and generator resistances may be specified by the designer whereas for the low-pass case optimum design occurs only for a specified load to generator impedance level ratio.

A bandpass filter is easily derived by the low-pass to bandpass frequency mapping

$$\frac{\omega'}{\omega'_c} = \frac{1}{w}\left(\frac{\omega}{\omega_o} - \frac{\omega_o}{\omega}\right) \tag{16}$$

where $\omega_o^2 = \omega_1\omega_2$ and $w = \dfrac{\omega_2 - \omega_1}{\omega_o}$. The low-pass frequency variable is ω' and the bandpass frequency variable is ω. The bandwidth of the bandpass filter is $\omega_2 - \omega_1$ and the center frequency is ω_o. This mapping transforms shunt capacitors into parallel resonant circuits and series inductors into series resonant circuits. Both of these types resonate at ω_o. The circuits of Figs. 1 and 2 are transformed into the bandpass circuits of Figs. 5 and 6.

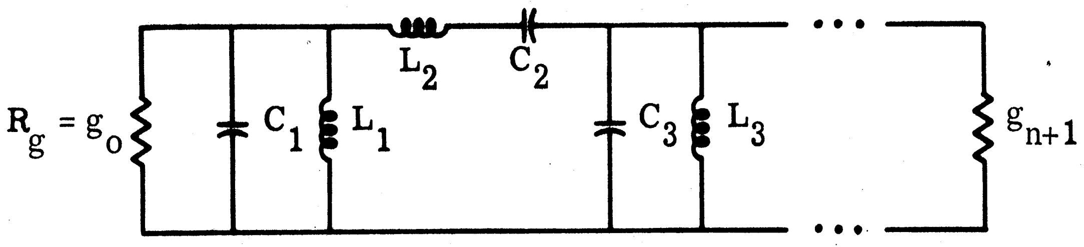

$$C_\ell = \frac{g_\ell \omega_c'}{\omega_o w} \qquad L_\ell = \frac{w}{\omega_o \omega_c' g_\ell} \qquad \text{(Shunt Reactances)}$$

$$C_\ell = \frac{w}{\omega_o \omega_c' g_\ell} \qquad L_\ell = \frac{g_\ell \omega_c'}{\omega_o w} \qquad \text{(Series Reactances)}$$

Fig. 5. Bandpass prototype starting with shunt resonator

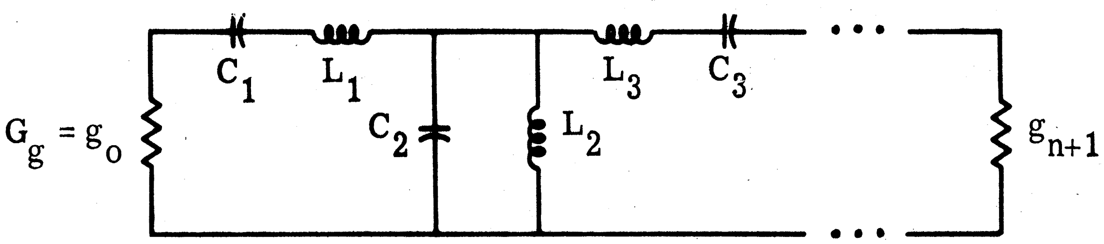

The element values are given by the same formulas found in Fig. 5.

Fig. 6. Bandpass prototype starting with series resonator

The steps are carried out in greater detail in several references (Ref. 5, pp. 356-362).

VI. Impedance Inverters

Many kinds of microwave filters can be constructed more conveniently if they can be built from either all capacitive or all inductive elements. This can be done with the use of ideal impedance or admittance inverters for the low-pass case. For the bandpass case, a filter may be constructed with only series or only shunt resonant circuits when inverters are used. The ideal impedance inverter is defined in Figs. 7(a) and (b).

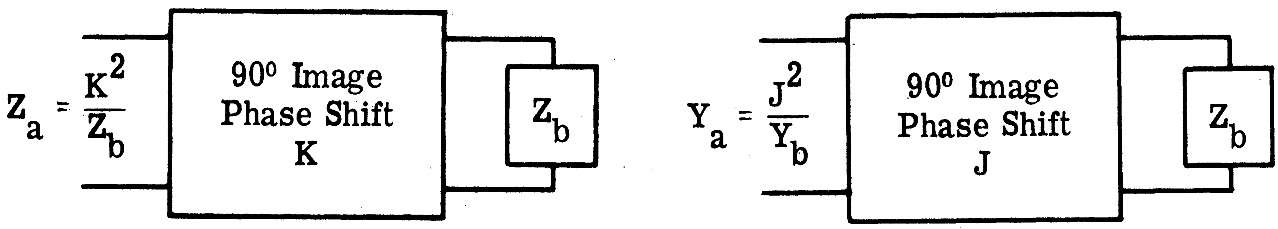

(a) K inverter (b) J inverter

Fig. 7. Ideal impedance inverters

One obvious example of a K inverter is a quarter wavelength of transmission line with a characteristic impedance of K at all frequencies.

The lumped bandpass filters shown in Figs. 5 and 6 may be built from series resonant circuits separated by K inverters or from shunt resonant circuits separated by J inverters as shown in Figs. 8 and 9.

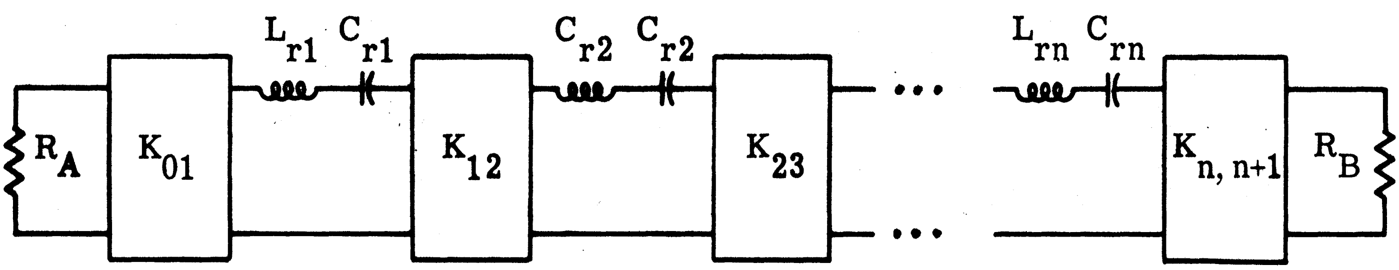

Fig. 8. Lumped bandpass impedance matching network using K inverters

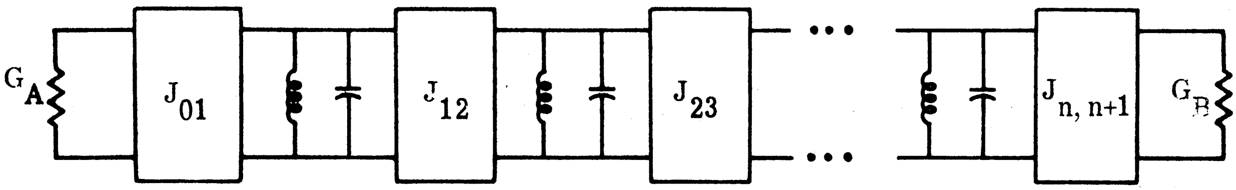

Fig. 9. Lumped bandpass impedance matching network using J inverters

The values of the $K_{i,\,i+1}$ are found on the basis that the circuit in Fig. 8 must have the same response as the circuit in Fig. 5. A section of the lumped prototype is given in Fig. 10 together with the equivalent section of the inverter network in Fig. 11.

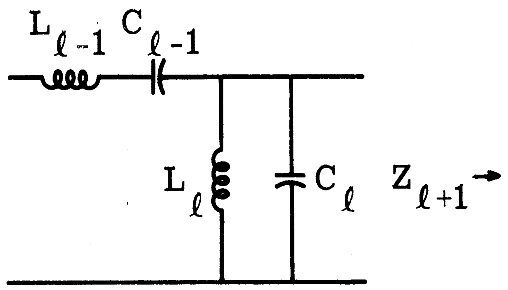

$$L_{\ell-1} = \frac{\omega'_c\, g_{\ell-1}}{\omega_o w} \qquad L_\ell = \frac{w}{\omega_o \omega'_c g_\ell}$$

$$C_{\ell-1} = \frac{w}{\omega_o \omega'_c g_{\ell-1}} \qquad C_\ell = \frac{\omega'_c\, g_\ell}{\omega_o w}$$

Fig. 10. Prototype section

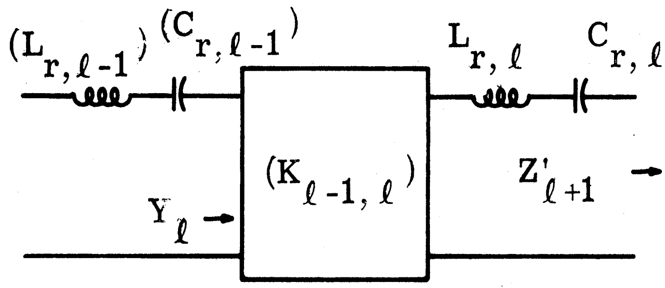

Fig. 11. K inverter section

The elements $L_{\ell-1}$ and $C_{\ell-1}$ constitute the left hand series arm needed for the circuit of Fig. 11, but the impedance level must be changed to correspond to that of Fig. 11. This is accomplished by multiplying all the inductances by $L_{r,\ell-1}/L_{\ell-1}$ and all capacitors by $L_{\ell-1}/L_{r,\ell-1}$ as indicated in Fig. 12.

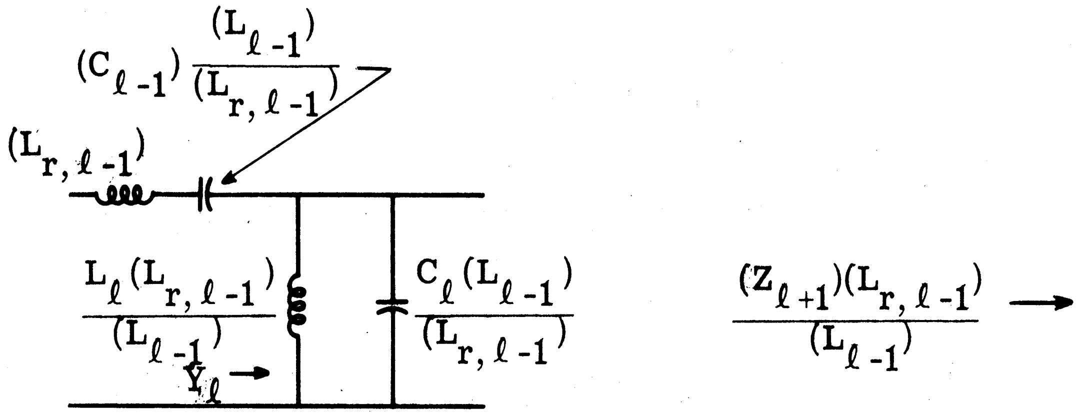

Fig. 12. Prototype with adjusted impedance level

For the circuit of Fig. 12 to be identical to that of Fig. 11, Y_ℓ must be the same for both.

$$\frac{K^2_{\ell-1,\ell}}{j[\omega L_{r,\ell} - 1/(\omega C_{r,\ell})] + Z'_{\ell+1}} = \frac{1}{j\left[\dfrac{\omega C_\ell(L_{\ell-1})}{(L_{r,\ell-1})} - \dfrac{(L_{\ell-1})}{\omega L_\ell(L_{r,\ell-1})}\right] + Y_{\ell+1}\dfrac{(L_{\ell-1})}{(L_{r,\ell-1})}}$$

$$K^2_{\ell-1}\left\{j\left[\omega\frac{C_\ell(L_{\ell-1})}{(L_{r,\ell-1})} - \frac{(L_{\ell-1})}{\omega L_\ell(L_{r,\ell-1})}\right] + (Y_{\ell+1})\frac{(L_{\ell-1})}{(L_{r,\ell-1})}\right\} \tag{17}$$

$$= j\left\{\omega L_{r,\ell} - 1/(\omega C_{r,\ell})\right\} + Z'_{\ell+1}$$

The terms with the same frequency dependence are equated to give a solution for K.

$$K_{\ell-1,\ell} = \sqrt{\frac{L_{r,\ell}(L_{r,\ell-1})}{(L_{\ell-1})C_\ell}} \quad \text{with } L_\ell C_\ell = L_{r,\ell}' C_{r,\ell} = \frac{1}{\omega_o^2} \tag{18}$$

The K can be written in terms of the original low-pass prototype by referring to Fig. 10.

$$K_{\ell,\ell+1} = \frac{\omega_o w}{\omega_c'} \sqrt{\frac{L_{r,\ell}(L_{r,\ell+1})}{g_\ell g_{\ell+1}}} \tag{19}$$

The first and last K's are obtained similarly. Figure 13 is the first section of the total bandpass circuit of Fig. 5.

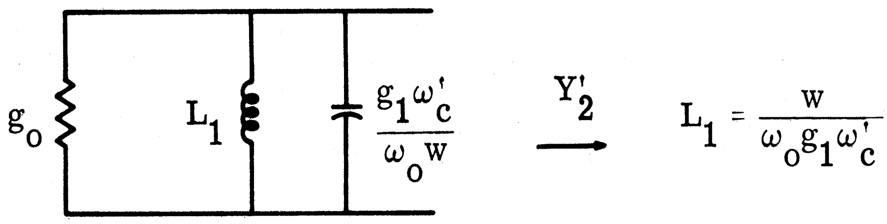

Fig. 13. Input section of prototype

The impedance level is raised to the desired generator resistance by multiplying all impedances by R_A/g_o as shown in Fig. 14.

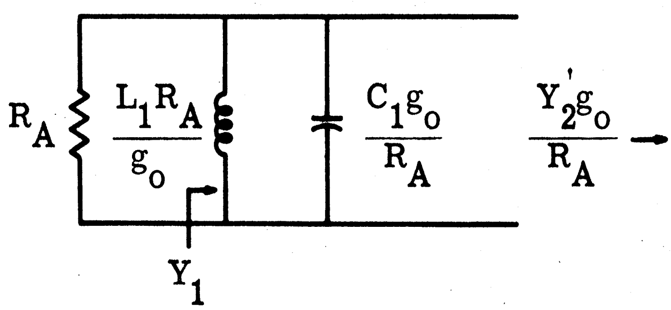

Fig. 14. Unnormalized input section of prototype

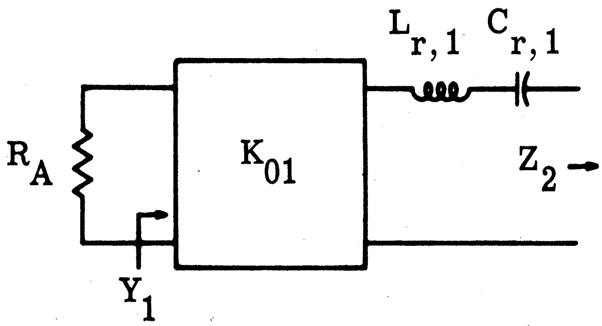

Fig. 15. Input K inverter section

This must have the same response as the network with the K inverter of Fig. 15 so Y_1 are the same in both cases.

$$j\left[\frac{g_o g_1 \omega_c' \omega}{\omega_o w R_A} - \frac{\omega_o \omega_c' g_o g_1}{\omega R_A w}\right] + Y_2' g_o / R_A = \frac{1}{K_{01}^2}\left\{ j\left[\omega L_{r,1} - \frac{1}{\omega C_{r,1}}\right] + Z_2 \right\} \tag{20}$$

$$K_{01} = \sqrt{\frac{\omega_o w L_{r,1} R_A}{\omega_c' g_o g_1}} \tag{21}$$

Similarly

$$K_{n,\,n+1} = \sqrt{\frac{\omega_o w\, L_{r,\,n} R_B}{\omega_c' g_n g_{n+1}}} \tag{22}$$

The bandpass prototype circuit of Fig. 5 can therefore be replaced by the circuit of Fig. 8 with its associated K inverters. Since the K or J inverters have the ability to shift the impedance levels, the sizes of the R_A and R_B as well as the $L_{r,\,\ell}$ may be chosen arbitrarily while retaining the same response as the prototype circuit. The use of K inverters has given the designer additional flexibility especially with regard to his choice of R_A and R_B.

VII. Microwave Realization

The parameters for the circuit of Fig. 8 have been explicitly derived, but two problems still remain for realization in a microwave structure: (1) how are the series resonant circuits to be made, and (2) how are the K inverters realized. Before actually resolving the first question it is convenient to generalize the expressions for the K's and corresponding J's to make them more compatible with distributive elements.

A series LC circuit or more generally a series resonator which has zero reactance at ω_o can be described in terms of its resonant frequency ω_o and a reactance slope parameter χ.

$$\chi = \frac{\omega_o}{2} \frac{dX}{d\omega}\bigg|_{\omega_o} \tag{23}$$

A shunt resonator where the susceptance is zero at ω_o, in turn can be described in terms of its resonant frequency and a susceptance slope parameter b.

$$b = \frac{\omega_o}{2} \frac{dB}{d\omega}\bigg|_{\omega_o} \tag{24}$$

For the series LC circuit $\chi = \omega_o L$ and for the shunt LC circuit $b = \omega_o C$. Thus the Q for a circuit with resistance R in series with a series resonator or a conductance G in parallel with a shunt resonator is $Q = \chi/R$ and $Q = b/G$ respectively. The K and J values in terms of these slope parameters are given in Figs. 16 and 17. For distributed circuits, these figures should be used rather than Figs. 8 and 9.

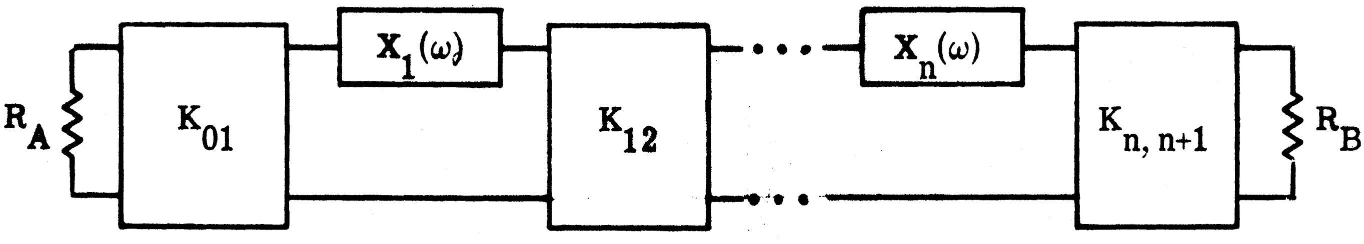

$$K_{01} = \sqrt{\frac{R_A w \chi_1}{g_0 g_1 \omega_c'}} \qquad K_{j,j+1} = \frac{w}{\omega_c'}\sqrt{\frac{\chi_j \chi_{j+1}}{g_j g_{j+1}}} \qquad K_{n,n+1} = \sqrt{\frac{R_B w \chi_n}{\omega_c' g_n g_{n+1}}}$$

$$j = 1, \ldots, n-1$$

Fig. 16. Generalized impedance matching networks using K inverters

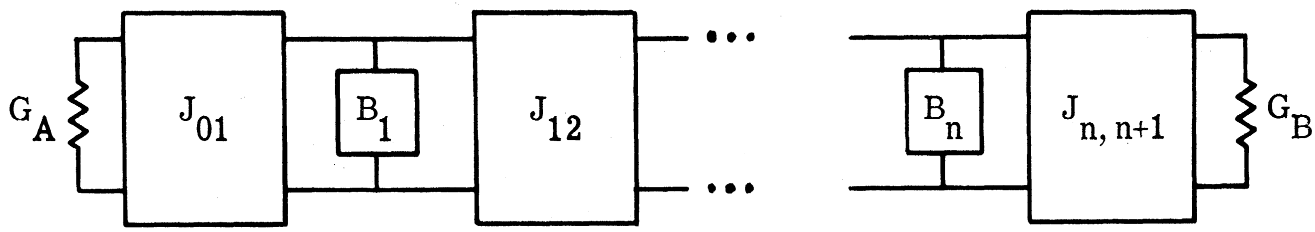

$$J_{01} = \sqrt{\frac{G_A b_1 w}{g_o g_1 \omega'_c}} \qquad J_{j,j+1} = \frac{w}{\omega'_c}\sqrt{\frac{b_j b_{j+1}}{g_j g_{j+1}}} \qquad J_{n,n+1} = \sqrt{\frac{G_B b_n w}{\omega'_c g_n g_{n+1}}}$$

$$j = 1, \ldots, n-1$$

Fig. 17. Generalized impedance matching network using J inverters

The series resonant circuits $X_i(\omega)$, shown in Fig. 16, can be realized as a half wavelength transmission line. Thus the choice of $L_{r,\ell}$ in the previous section is equivalent to the choice of characteristic impedance of the half wavelength line. Often all the X_i can be made to have the same characteristic impedance of 50 ohms. The reactance slope parameter is obtained from the transmission line equation. The reactance of the transmission line is

$$X = Z_o \frac{(Z_o^2 - R_L^2) \tan \phi}{Z_o^2 + R_L^2 \tan^2 \phi} \tag{25}$$

where $\phi = \beta d = \omega d/c$. The slope parameter is obtained by differentiation of X.

$$\chi = Z_o \frac{\omega_o}{2} (Z_o^2 - R_L^2) \frac{d}{c} \sec^2 \phi \frac{Z_o^2 + R_L^2 \tan^2 \phi - 2R_L^2 \tan^2 \phi}{(Z_o^2 + R_L^2 \tan^2 \phi)^2}$$

$$\chi = \frac{Z_o}{2} \frac{\omega_o d}{c} (Z_o^2 - R_L^2) \sec^2 \phi \frac{Z_o^2 - R_L^2 \tan^2 \phi}{(Z_o^2 + R_L^2 \tan^2 \phi)^2} \tag{26}$$

For a transmission line resonant at $\phi = \pi$

$$\chi = \frac{Z_o \pi}{2} \left(\frac{Z_o^2 - R_L^2}{Z_o^2} \right) \tag{27}$$

Inversion networks often present a very small resistance in shunt with the series resonator so that $R_L / Z_o << 1$. In this case

$$\chi \cong \frac{Z_o \pi}{2} \tag{28}$$

The impedance matching properties of a series of K inverters can be shown by an example. In Fig. 18 two unequal resistances are matched with three K inverters separated by half-wavelength transmission-lines.

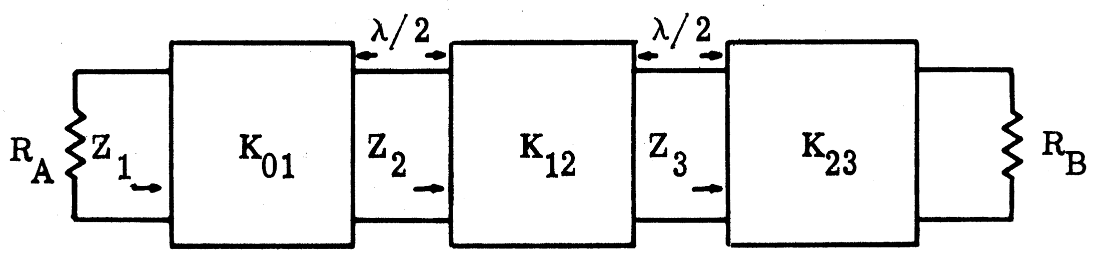

Fig. 18. Three K inverter example

Each K inverter inverts the impedance.

$$Z_3 = \frac{K_{23}^2}{R_B}$$

$$Z_2 = \frac{K_{12}^2 R_B}{K_{23}^2}$$

$$Z_1 = \frac{K_{01}^2 K_{23}^2}{K_{12}^2 R_B}$$

Using the values of the K's from Fig. 16,

$$Z_1 = \frac{R_A w \chi_1}{g_o g_1 \omega_c'} \cdot \frac{R_B w \chi_2}{g_2 g_3 \omega_c'} \cdot \frac{\left(\omega_c'\right)^2 g_1 g_2}{w^2 \chi_1 \chi_2} \cdot \frac{1}{R_B}$$

$$Z_1 = \frac{R_A}{g_o g_3}$$

In general with n K inverters, the input impedance is $Z_1 = \frac{R_A}{g_o g_{n+1}}$ when n is even and $\frac{R_A g_{n+1}}{g_o}$ when n is odd. The parameter g_o is always chosen as 1 while $g_{n+1} \neq 1$ for Chebyshev filters when n is even or for Chebyshev impedance matching networks when the load is complex. If $g_{n+1} \neq 1$ the designer must modify the value of R_A in K_{01} so as to obtain the correct impedance level.

The series resonant circuits can be realized in a microwave structure by a half-wavelength transmission line with a reactance slope parameter of $\pi Z_0/2$. The second question needing clarification is how the K inverters are realized. One inverter already mentioned is a quarter wavelength line. Much broader bandwidth may be achieved using the K inverters in Fig. 19 or the J inverters in Fig. 20.

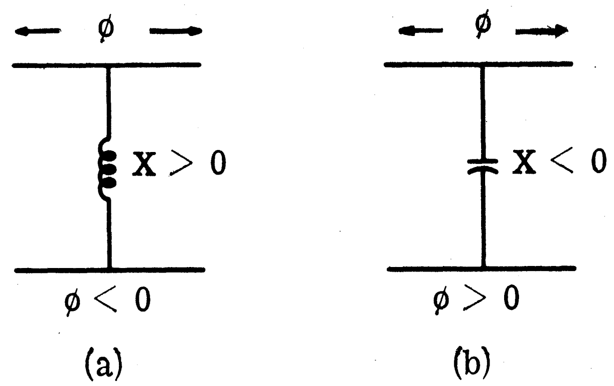

Fig. 19. Lumped K inverter realization

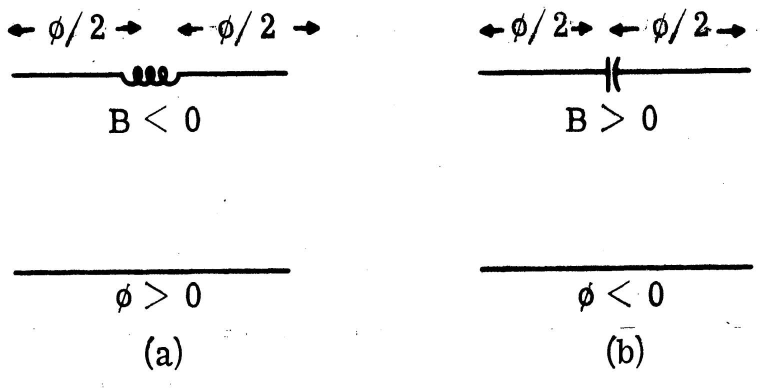

Fig. 20. Lumped J inverter realization

In Figs. 19(a) and 20(b) the negative line length must be absorbed by available line length between inverters. The value of K for the inverters of Fig. 19 is

$$K = Z_0 \tan |\phi/2| \tag{29}$$

where

$$\phi = - \text{Arctan} \, (2X/Z_o) \tag{30}$$

$$X/Z_o = \frac{K/Z_o}{1 - (K/Z_o)^2} \tag{31}$$

The value of J for the J inverters in Fig. 20. is

$$J = Y_o \tan |\phi/2| \tag{32}$$

where

$$\phi = - \text{Arctan} \, 2B/Y_o \tag{33}$$

$$B/Y_o = \frac{J/Y_o}{1 - (J/Y_o)^2} \tag{34}$$

Thus when K or J is calculated by the equations in Figs. 16 or 17, ϕ and the reactance or susceptance can be found. The derivation of these formulas may be found in Cohn's work (Ref. 1) and will not be rederived here. A more general set of relations based on Fig. 19(b) will be derived later which give the above results when specialized to a lumped capacitor.

VIII. Combining K and J Inverters

When wavelengths are too long to space inverters of one kind every half wavelength, K and J inverters can be placed alternately every quarter wavelength as in Fig. 21.

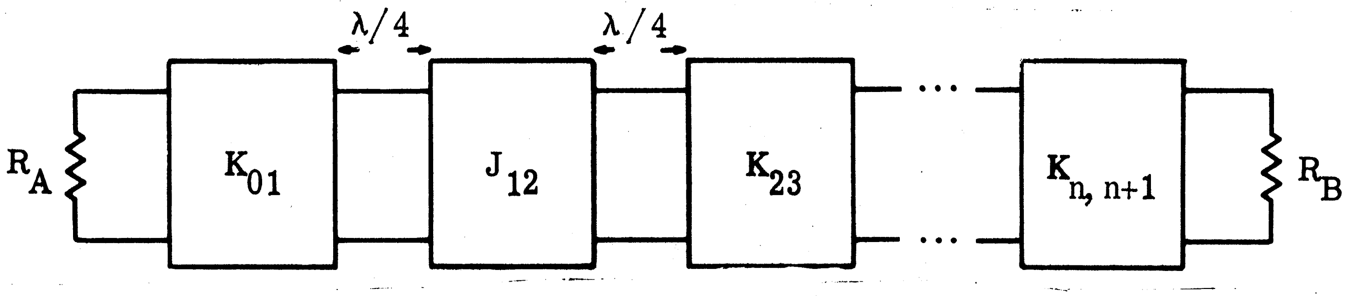

Fig. 21. Alternate K and J inverters

The only difference between the values here and those in Figs. 16 and 17 is a difference in slope parameter. For a quarter wavelength line $\chi = \pi Z_o / 4$ and $b = \pi Y_o / 4$.

IX. K Inverter with Disks of Nonzero Length

The image impedance and the image propagation function are found useful in the derivation of the disk length and phase shift of the impedance inverter. The image impedance in a uniform transmission line is the characteristic impedance of the line, and the image propagation function is the propagation constant of the transmission line. The image impedance and propagation function are more general than that implied above for a uniform line. If Z_{I1} and Z_{I2} are the image impedances of an unsymmetrical network, then an infinite chain of these networks connected together, as shown in Fig. 22, will present its corresponding image impedance at any junction of these networks.

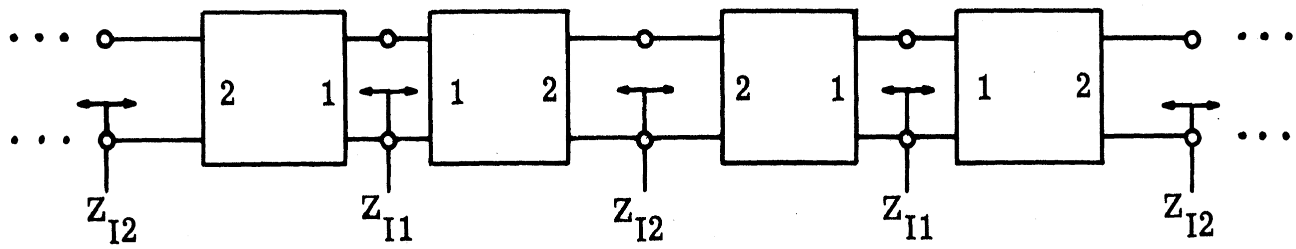

Fig. 22. Image impedance for Z_{I1} infinite network chain

Since the impedance is the same in both directions, the reflection coefficient at each junction is zero. If a wave propagates from left to right, its phase and attenuation will be affected by each network according to its image propagation function, but it will travel from one network to another without reflection (Ref. 4, pp. 49-50).

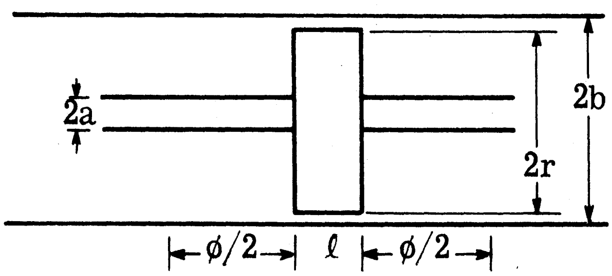

Fig. 23. Coaxial realization of the K inverter of Fig. 19(b)

The design of the K inverters used in the previous designs is based on one of Cohn's procedures (Ref. 1), which is here designated as a "lumped-design procedure." In that procedure, the filter design calls for a K inverter of the form shown in Fig. 23. The inverter is realized by selecting a disk of nonzero length, so that the disk capacitance is equal to that of the capacitor in Fig. 19(b).

A more accurate procedure has been developed here, and is designated as a "distributed-design procedure." This procedure follows the general form of Cohn's analysis, but considers the coaxial K inverter shown in Fig. 23 to be a section of low-Z_o line rather than a lumped capacitor. The dimensions of this structure are thus chosen with regard to the distributed character of the disk. Typically, the disk diameter is specified, and the length and characteristic impedance are determined.

The image propagation constant can be expressed as

$$\tanh \gamma = \sqrt{\frac{1}{Z_{11} Y_{11}}} = \sqrt{\frac{Z_{sc}}{Z_{oc}}}$$

and the image impedance as

$$Z_{I1} = K = \sqrt{\frac{Z_{11}}{Y_{11}}} = \sqrt{Z_{oc} Z_{sc}}$$

$Z_{11} = Z_{oc}$ is the input impedance of a two-port network when the output is open circuited, and $Y_{11} = 1/Z_{sc}$ is the input admittance of a two-port network when the output is short circuited (Ref. 3, pp. 186-191).

If the circuit element is bisected, as shown in Fig. 24, the open circuit and short circuit impedances can readily be found.

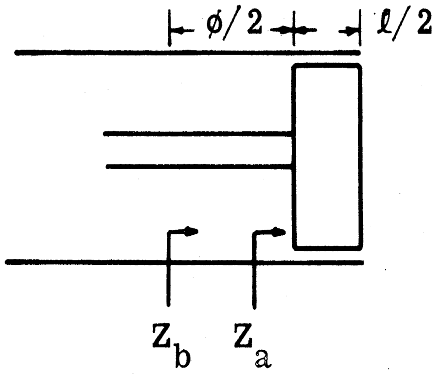

Fig. 24. Bisected disk element

For the open circuit case

$$Z_{aoc} = -jZ_c \cot \frac{\beta \ell}{2}$$

where $\beta = (\omega/c)\sqrt{\epsilon_r}$, and ϵ_r is the relative dielectric constant of the material between the disk and the outer conductor while Z_c is the characteristic impedance of the coaxial disk. Now Z_{aoc} is translated a distance $\phi/2$ down the coaxial line (which has characteristic impedance Z_o). Since this circuit is assumed lossless, the impedance at Z_b is imaginary.

$$X_{boc} = Z_o \frac{\tan \phi/2 - \frac{Z_c}{Z_o} \cot \frac{\beta \ell}{2}}{1 + \frac{Z_c}{Z_o} \cot \frac{\beta \ell}{2} \tan \frac{\phi}{2}}$$

This can be expressed as the tangent of the sum of two angles by a trigonometric identity.

$$X_{boc} = Z_o \tan\left[\frac{\phi}{2} - \text{Arctan}\left(\frac{Z_c}{Z_o}\cot\frac{\beta\ell}{2}\right)\right]$$

If instead of an open circuit, as shown in Fig. 24, there is a short circuit at the plane of bisection, then

$$Z_{asc} = jZ_c \tan\frac{\beta\ell}{2}$$

Translating this $\phi/2$ radians, the short circuit reactance is found.

$$X_{bsc} = Z_o \tan\left[\frac{\phi}{2} + \text{Arctan}\left(\frac{Z_c}{Z_o}\tan\frac{\beta\ell}{2}\right)\right]$$

Since this circuit is lossless, the propagation constant consists of only the imaginary part β'.

$$-j\gamma = \beta' = 2\,\text{Arctan}\sqrt{\frac{-X_{bsc}}{X_{boc}}}$$

$$\beta' = 2\,\text{Arctan}\left\{\frac{-Z_o \tan\left[\frac{\phi}{2} + \text{Arctan}\left(\frac{Z_c}{Z_o}\tan\frac{\beta\ell}{2}\right)\right]}{Z_o \tan\left[\frac{\phi}{2} - \text{Arctan}\left(\frac{Z_c}{Z_o}\cot\frac{\beta\ell}{2}\right)\right]}\right\}^{1/2}$$

As in the quarter-wave transformer, the electrical length is $\beta' = \pm 90^0$.

This means the argument of the Arctan is 1.

$$\tan\left[-\frac{\phi}{2} - \text{Arctan}\left(\frac{Z_c}{Z_o}\tan\frac{\beta\ell}{2}\right)\right] = \tan\left[\frac{\phi}{2} - \text{Arctan}\left(\frac{Z_c}{Z_o}\cot\frac{\beta\ell}{2}\right)\right] \tag{35}$$

$$\phi = \text{Arctan}\left(\frac{Z_c}{Z_o}\cot\frac{\beta\ell}{2}\right) - \text{Arctan}\left(\frac{Z_c}{Z_o}\tan\frac{\beta\ell}{2}\right)$$

Using the trigonometric identity, Arctan A $\pm$ Arctan B = Arctan $[(A \pm B)/(1 \mp AB)]$, the phase angle ϕ may be expressed in terms of the yet unknown length ℓ.

$$\phi = \text{Arctan}\left[\frac{\frac{Z_c}{Z_o}\left(\cot\frac{\beta\ell}{2} - \tan\frac{\beta\ell}{2}\right)}{1 + \left(\frac{Z_c}{Z_o}\right)^2}\right] \tag{36}$$

If $\beta\ell/2 << 1$, this ϕ reduces to the value obtained by Cohn as indicated in Eq. 30.

The image impedance or K value can be found also.

$$K = \sqrt{-X_{boc}\, X_{bsc}}$$

$$K = Z_o\sqrt{\tan\left[-\frac{\phi}{2} + \text{Arctan}\left(\frac{Z_c}{Z_o}\cot\frac{\beta\ell}{2}\right)\right]\tan\left[\frac{\phi}{2} + \text{Arctan}\left(\frac{Z_c}{Z_o}\tan\frac{\beta\ell}{2}\right)\right]}$$

Eliminating the cotangent term by use of Eq. 35 gives the value of K in terms of the unknown length ℓ.

$$K = Z_o \tan\left[\frac{\phi}{2} + \operatorname{Arctan}\left(\frac{Z_c}{Z_o}\tan\frac{\beta\ell}{2}\right)\right] \tag{37}$$

This again reduces to Cohn's value for K in Eq. 29 when $\beta\ell/2 = 0$. An expression for $\phi/2$ in terms of K is found by applying the trigonometric identity for the tangent of the sum of two angles to Eq. 37.

$$\frac{K}{Z_o} = \frac{\tan\frac{\phi}{2} + \frac{Z_c}{Z_o}\tan\frac{\beta\ell}{2}}{1 - \tan\left(\frac{\phi}{2}\right)\left(\frac{Z_c}{Z_o}\tan\frac{\beta\ell}{2}\right)}$$

Solving this for $\phi/2$ gives

$$\tan\frac{\phi}{2} = \frac{\frac{K}{Z_o} - \frac{Z_c}{Z_o}\tan\frac{\beta\ell}{2}}{1 + \frac{KZ_c}{Z_o^2}\tan\frac{\beta\ell}{2}} \tag{38}$$

Equations 36 and 38 are two equations in the two unknowns ϕ and ℓ. The unknown ϕ will be eliminated, and the result will be one equation in the unknown $F \triangleq \tan\beta\ell/2$.

From Eq. 36

$$\tan \phi = \frac{\frac{Z_c}{Z_o}\left(\frac{1}{F} - F\right)}{1 + \left(\frac{Z_c}{Z_o}\right)^2} = \frac{2 \tan \frac{\phi}{2}}{1 - \tan^2 \frac{\phi}{2}}$$

Equation 38 is substituted into the right-hand side of the above expression.

$$\frac{\frac{Z_c}{Z_o}\left(\frac{1}{F} - F\right)}{1 + \left(\frac{Z_c}{Z_o}\right)^2} = \frac{2\left(\frac{K}{Z_o} - \frac{Z_c}{Z_o} F\right)\left(1 + \frac{KZ_c}{Z_o^2} F\right)}{1 + \frac{2KZ_c}{Z_o^2} F + \frac{K^2Z_c^2}{Z_o^4} F^2 - \frac{K^2}{Z_o^2} + \frac{2Z_cK}{Z_o^2} F - \left(\frac{Z_c}{Z_o}\right)^2 F^2}$$

This is a quartic equation which after some algebra can be written in the following form:

$$G^4 - 2\frac{K}{Z_c} PG^3 + \left[1 + \left(\frac{Z_c}{Z_o}\right)^2\right] G^2 - \frac{2KZ_c}{Z_o^2} PG + \left(\frac{Z_c}{Z_o}\right)^2 = 0$$

Here it is found convenient to define $F \triangleq 1/G$ and

$$P \triangleq \frac{1 - (Z_c/Z_o)^2}{1 - (K/Z_o)^2} \tag{39}$$

It should be noted that P is normally positive. This expression can be factored to give four roots.

$$G = \pm j \frac{Z_c}{Z_o}$$

$$G = \frac{KP}{Z_c} \pm \sqrt{\left(\frac{KP}{Z_c}\right)^2 - 1}$$

The second two roots are the roots of interest. The reciprocal of G gives an explicit solution for ℓ in terms of known quantities.

$$\frac{1}{G} = F = \tan\frac{\beta \ell}{2} = \frac{KP}{Z_c} \pm \sqrt{\left(\frac{KP}{Z_c}\right)^2 - 1} \qquad (40)$$

X. J Inverter with Nonzero Inductor Length

The same general theory described in the previous section may be applied in an analogous fashion to the series inductor J inverter shown in Fig. 25.

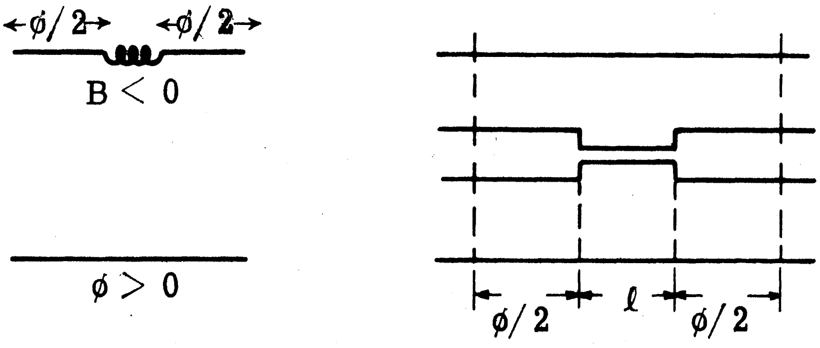

(a) Lumped J inverter (b) Distributed J inverter

Fig. 25. The series J inverter

In this case the image propagation constant is

$$\tanh\gamma = \sqrt{\frac{1}{Z_{11}Y_{11}}} = \sqrt{\frac{Y_{oc}}{Y_{sc}}}$$

and the image admittance is

$$Y_{I1} = J = \sqrt{\frac{Y_{11}}{Z_{11}}} = \sqrt{Y_{sc}Y_{oc}}$$

The derivation follows exactly as before with Z_{sc} replaced by Y_{oc}, Z_{oc} replaced by Y_{sc}, Z_c replaced by Y_c and Z_o replaced by Y_o. The final answer is

$$\tan\frac{\beta \ell}{2} = \frac{JP}{Y_c} \pm \sqrt{\left(\frac{JP}{Y_c}\right)^2 - 1} \qquad (40')$$

where

$$P = \frac{1 - (Y_c/Y_o)^2}{1 - (J/Y_o)^2} \qquad (39')$$

and

$$\phi = \text{Arctan}\left\{\frac{[\cot(\beta\ell/2) - \tan(\beta\ell/2)]\ (Y_c/Y_o)}{1 + (Y_c/Y_o)^2}\right\} \qquad (36')$$

The remaining two impedance inverters shown in Figs. 19(a) and 20(b) are not amenable to this kind of analysis since a structure approximating a shunt inductance or a series capacitance would not be a TEM structure.

XI. Effects of Discontinuity Capacitance

A sudden change in diameter of the center conductor introduces fringing capacitance which has not yet been accounted for in the design. Also higher order propagating and evanescent modes around the disks will have the effect of storing more energy than the theory presented would indicate. P. I. Somlo (Ref. 6) has derived curves for discontinuity capacitance which takes both these effects into account. For computer calculations he has given the approximate formula

$$C_d = \epsilon_o \cdot 2b \cdot \left[\frac{\alpha^2 + 1}{\alpha} \ln \frac{1 + \alpha}{1 - \alpha} - 2 \ln \frac{4\alpha}{1 - \alpha^2} \right]$$

$$+ 0.111 \cdot (1 - \alpha)(\tau - 1) \cdot 2\pi \cdot b \cdot 10^{-12} \qquad (41)$$

where b is the radius of the outside conductor, a is the radius of the center conductor, r is the radius of the disk, $\alpha = (b - r)/(b - a)$ and $\tau = b/a$. This formula introduces a maximum error of $\pm 0.03\ (2\pi b)$ pF when $0.01 \leq \alpha \leq 1.0$ and $1.0 \leq \tau \leq 6.0$.

The length of the disks must be shortened to account for this added capacitance. The capacitance of a TEM line is

$$C = \frac{\sqrt{\mu_o \epsilon}\ \ell'}{Z_c} \qquad (42)$$

where Z_c is the characteristic impedance of the line at the disk given by

$$Z_c = \frac{1}{2\pi}\sqrt{\frac{\mu_o}{\epsilon}} \ln (b/r) \tag{43}$$

Since there are two discontinuities for the disk, the total discontinuity capacitance $C = 2\,C_d$ and the length ℓ' by which the disk must be shortened is easily found.

For the case of the series inductor J inverter, the shunt discontinuity capacitance cannot be absorbed in the inductor as is possible for the disk K inverter.

XII. Design Procedure

The procedure for the design of a disk K inverter for a bandpass filter in a coaxial line follows:

(1) A value for K is calculated on the basis of the formulas under Fig. 16. Usually tables for the g_j are normalized so that $\omega'_c = 1$.

(2) A diameter is assumed for the disk. The larger the disk diameter, the smaller its length will be, and the greater its discontinuity capacitance.

(3) The disk characteristic impedance is found from the relation 43 (Ref. 2, p. 81) where "r" is the center conductor (in this case, disk) radius and "b" is the outer conductor radius.

(4) The value for P is found from Eq. 39.

(5) At this point a test must be made. If the value $KP/Z_c < 1$, the disk diameter is too small, and a larger one must be assumed.

(6) Use Eq. 40 to find the disk length.

(7) Use Eq. 36 or 38 to find the phase angle ϕ.

(8) The discontinuity capacitance is found from Eq. 41 and a length ℓ' from Eq. 42 is subtracted from the disk length.

The disk length found in step 6 must of course be larger than ℓ'. The assumed disk diameter, and the resulting disk length and phase angle completely specify the disk K inverter. This design approach accounts for the nonzero disk length.

XIII. 50-Ohm to 50-Ohm Bandpass Filters

Several curves were derived for various bandpass filters centered at 8.5 GHz with different fractional bandwidths for the purpose of comparing the distributed design described in the previous section with the lumped design. The following filters were based on a Chebyshev low-pass prototype circuit with 0.1 dB ripple. For the three-ripple case this means that $g_0 = 1.0$, $g_1 = 1.0315$, $g_2 = 1.474$, $g_3 = 1.0315$, and $g_4 = 1.0$. The design was carried out using 50-ohm coaxial line with an outer conductor diameter of 0.5626 in. and a center conductor diameter of 0.24425 in. In the theoretical curves which follow, the effect of discontinuity capacitance has been neglected. However, when a coaxial bandpass filter is built, the design should be modified to account for the discontinuity capacitance as described in Section XII. Figures 26, 27, and 28 show that there is considerable improvement in using the distributed design. The distributed design filters are all centered at the design frequency although the bandwidth is narrower than the design bandwidth. The maximum ripple in the passband is smaller for the distributed case although it is still larger than the design ripple of 0.1 dB or $|\Gamma|^2 = 0.023$.

The design data for these curves are shown in Table I. Since the bandpass filter is symmetrical, the first two disks are identical with the last two, so only the values for the first two are given.

XIII a. Six-Disk Filter Using Distributed Design. A 5-percent and a 10-percent bandwidth filter were designed with six disks using the distributed design technique. The resulting curves are shown in Figs. 29 and 30. The same improvements over the lumped design are evident for the five-ripple case. A comparison of the five-ripple case and the three-ripple case for the distributed design shows that the maximum ripple is still higher for the five-ripple case.

The design parameters for the filters are shown in Table II. Since the filter is symmetrical, the first three disks are identical to the last three.

Tables I and II show that the difference in disk lengths between the lumped and distributed case is not large. As would be expected, the difference in the phase angles ϕ between the two cases is greatest

Lumped or Distributed	Bandwidth w	K_1	K_2	Disk Diameter D_1 in.	Disk Diameter D_2 in.	ℓ_1 cm	ℓ_2 cm	ϕ_1 rad.	ϕ_2 rad.
L	1%	6.1701	0.72194	0.502	0.554	0.3011	0.3496	0.24556	0.02888
D	1%	"	"	"	"	0.3471	0.4302	0.15534	0.01330
L	5%	13.7969	3.6097	0.502	0.532	0.1263	0.2547	0.53847	0.14414
D	5%	"	"	"	"	0.1298	0.2777	0.50663	0.10963
L	10%	19.5117	7.2193	0.502	0.502	0.0820	0.2559	0.74412	0.28679
D	10%	"	"	"	"	0.0833	0.2816	0.72378	0.21529

Table I. Disk parameters for bandpass filters with three ripples

Lumped or Distributed	Bandwidth w	K_1	K_2	K_3	D_1 in.	D_2 in.	D_3 in.
L	5%	13.0849	3.1316	2.3863	0.502	0.532	0.532
D	5%	"	"	"	"	"	"
L	10%	18.5049	6.2632	4.7726	0.502	0.502	0.532
D	10%	"	"	"	"	"	"

Lumped or Distributed	Bandwidth w	ℓ_1 cm	ℓ_2 cm	ℓ_3 cm	ϕ_1 rad.	ϕ_2 rad.	ϕ_3 rad.
L	5%	0.1343	0.2940	0.3864	0.51192	0.12510	0.09538
D	5%	0.1384	0.3328	0.5462	0.47793	0.82929	0.01747
L	10%	0.0880	0.2965	0.1919	0.70893	0.24923	0.19033
D	10%	0.0896	0.3399	0.2009	0.68706	0.16114	0.16587

Table II. Disk parameters for bandpass filters with five ripples

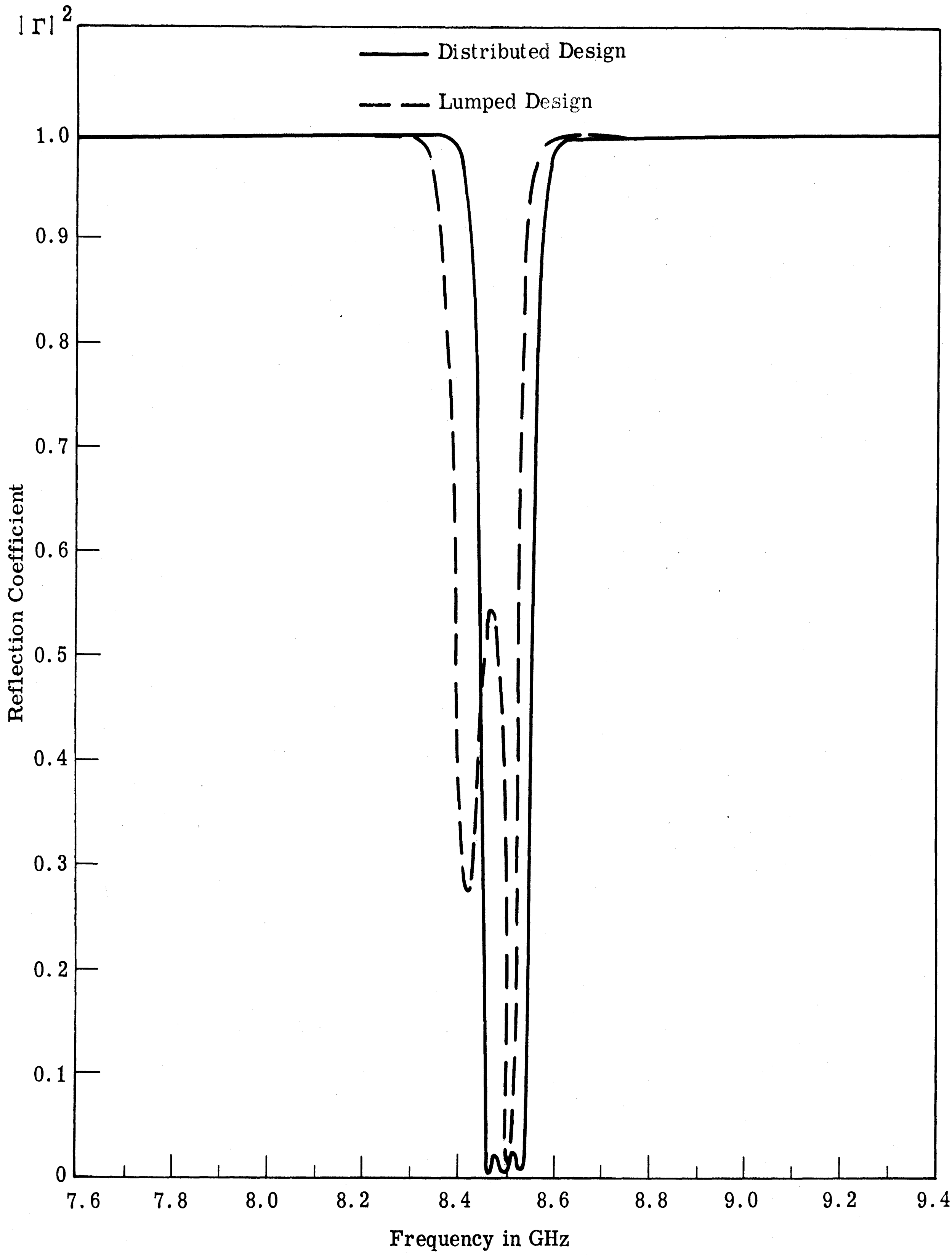

Fig. 26. Theoretical comparison between two design techniques for a 1 percent bandwidth bandpass filter which operates between two 50-ohm loads

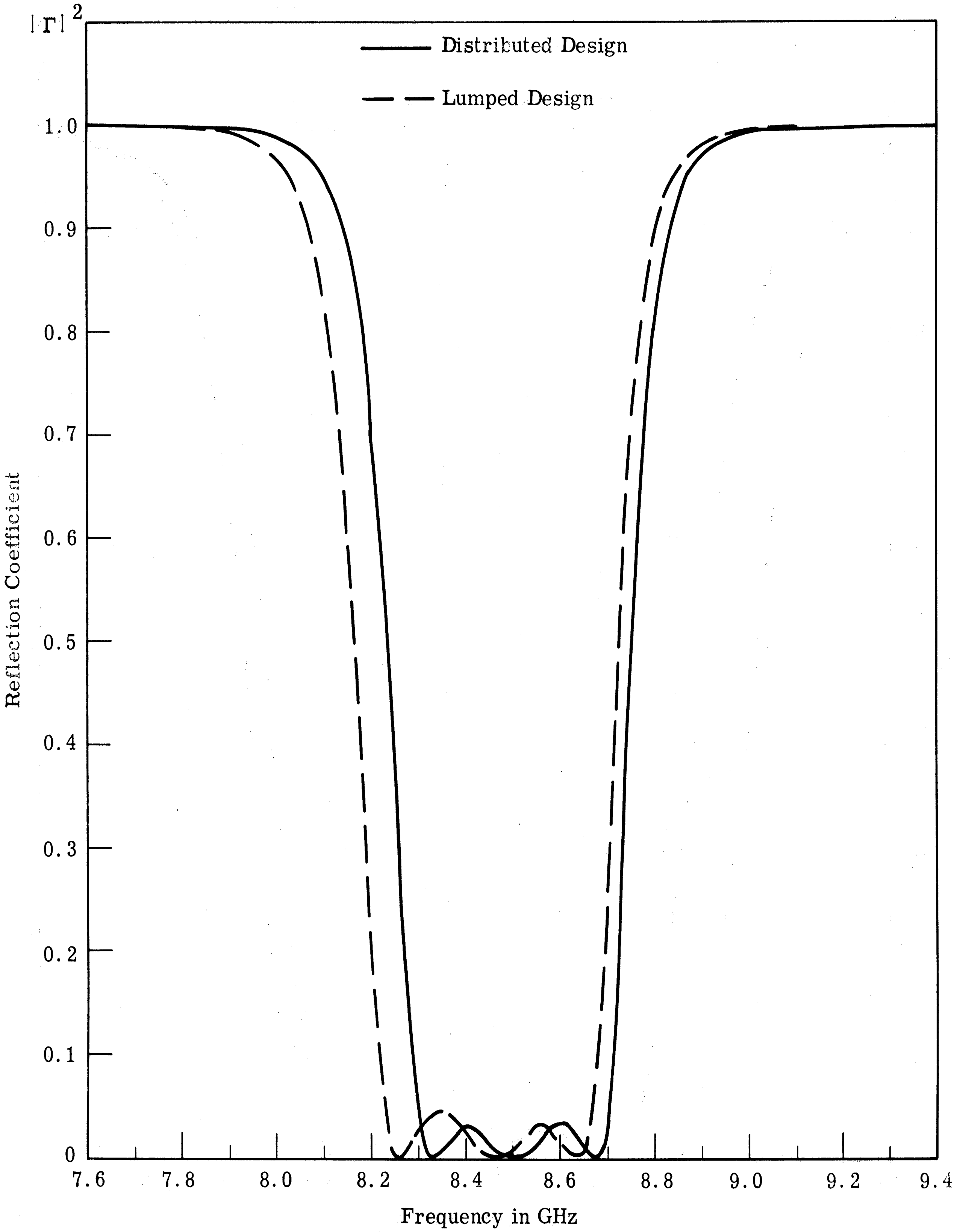

Fig. 27. Theoretical comparison between two design techniques for a 5 percent bandwidth bandpass filter which operates between two 50-ohm loads

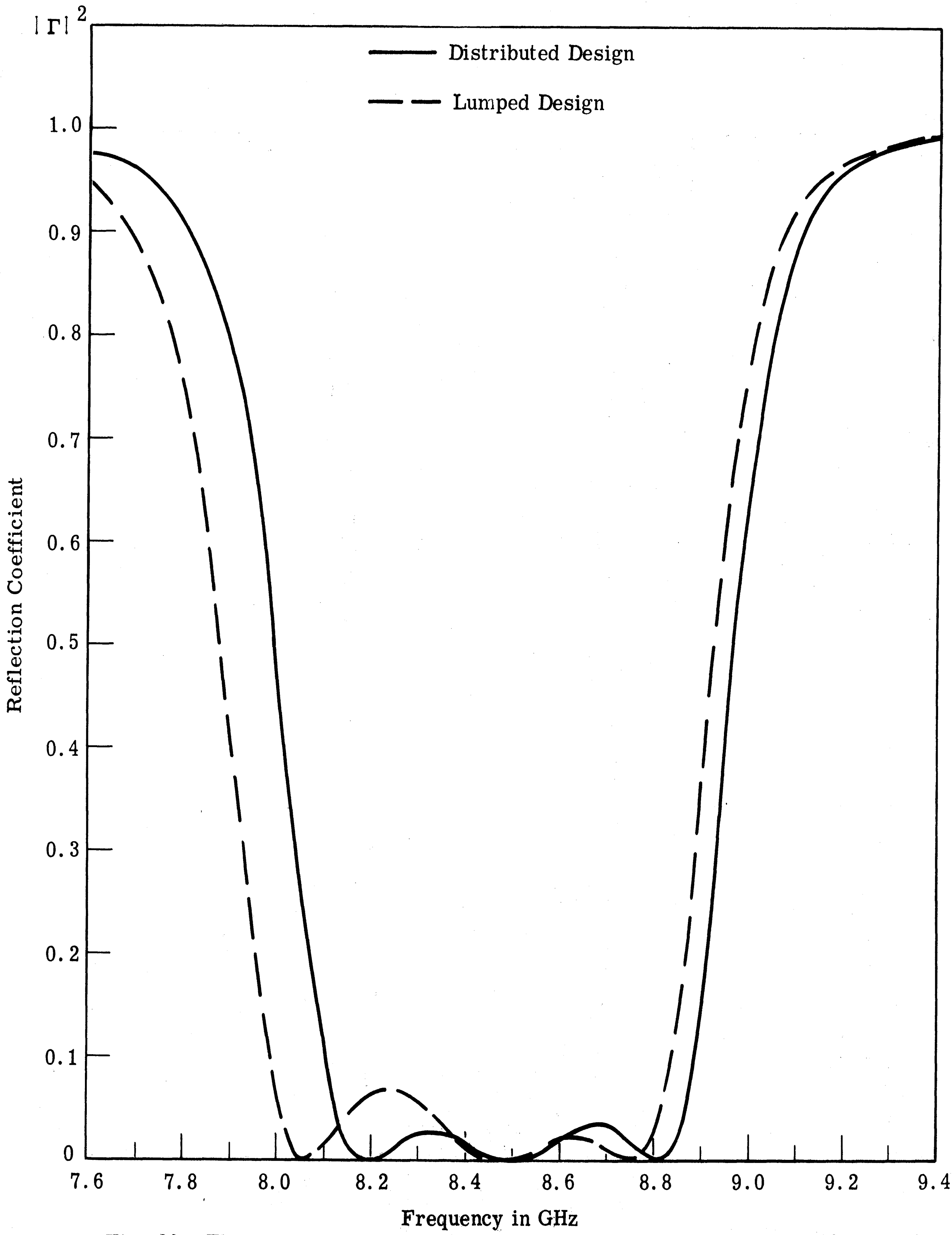

Fig. 28. Theoretical comparison between two design techniques for a 10 percent bandwidth bandpass filter which operates between two 50-ohm loads

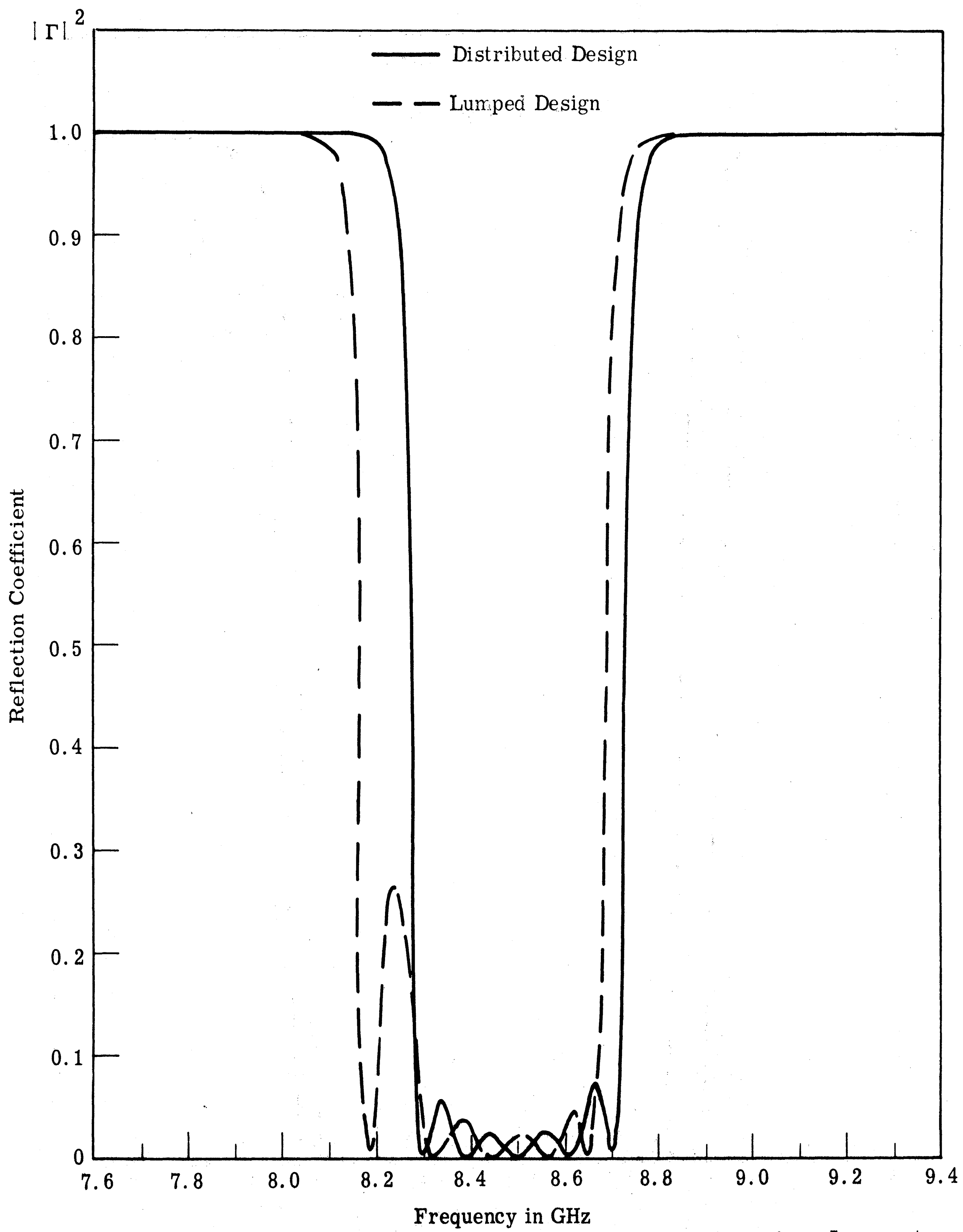

Fig. 29. Theoretical comparison between two design techniques for a 5 percent bandwidth 5-ripple filter which operates between two 50-ohm loads

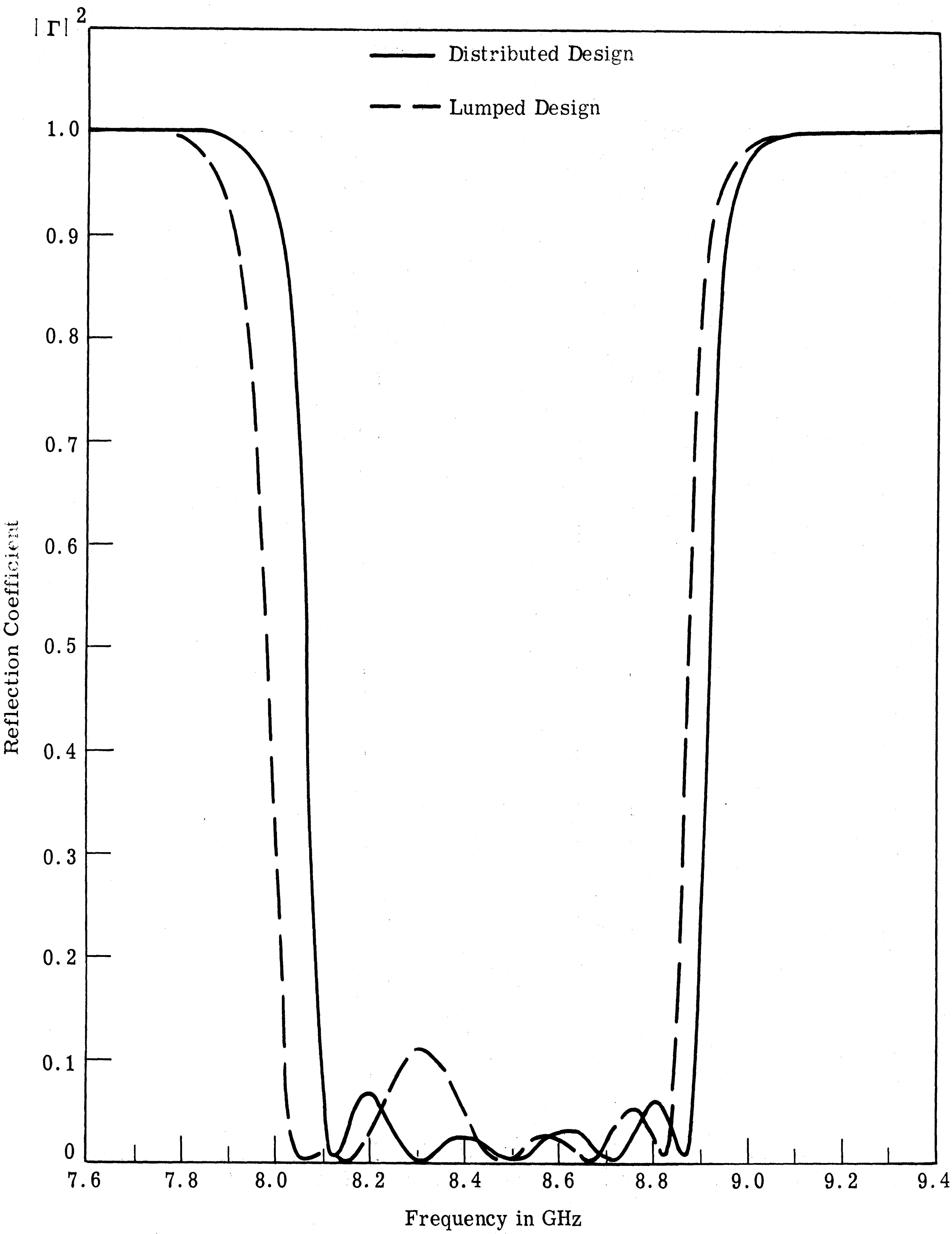

Fig. 30. Theoretical comparison between two design techniques for a 10 percent bandwidth 5-ripple filter which operates between two 50-ohm loads

when the disk length is large. The different disk diameters used in Tables I and II were the result of increasing the diameter to make the expression for $\tan \beta \ell / 2$ real.

XIII b. Impedance Transformer. The distributed design approach was used to design an impedance transformer operating between 50 ohms and a complex load whose real part was 1 ohm. The load was resonated with an appropriate reactance so that the resonated Q was Q_A. The load was assumed to have a Q_A such that the decrement δ was constant.

$$\delta = \frac{1}{wQ_A} = \frac{1}{17.5} = 0.0571$$

In this case the load acts as the first series resonator so the first K inverter is K_{12} which is given by

$$K_{12} = \frac{1}{\omega_c'} \sqrt{\frac{wR_A \chi_2}{g_1 g_2 \delta}}$$

The low-pass prototype g values can be obtained from a graph (Ref. 4, p. 128), and the values for K can be found from the above expression and the formulas found in Fig. 16. For an n pole low-pass prototype circuit, only n K inverters are needed for the matching network whereas n + 1 K inverters were needed for the 50-ohm to 50-ohm filter.

The results of the 50:1 impedance transformers are shown in Figs. 31 through 34 for different bandwidths. Again the passband was centered around f_0 for the distributed design case. The distributed design

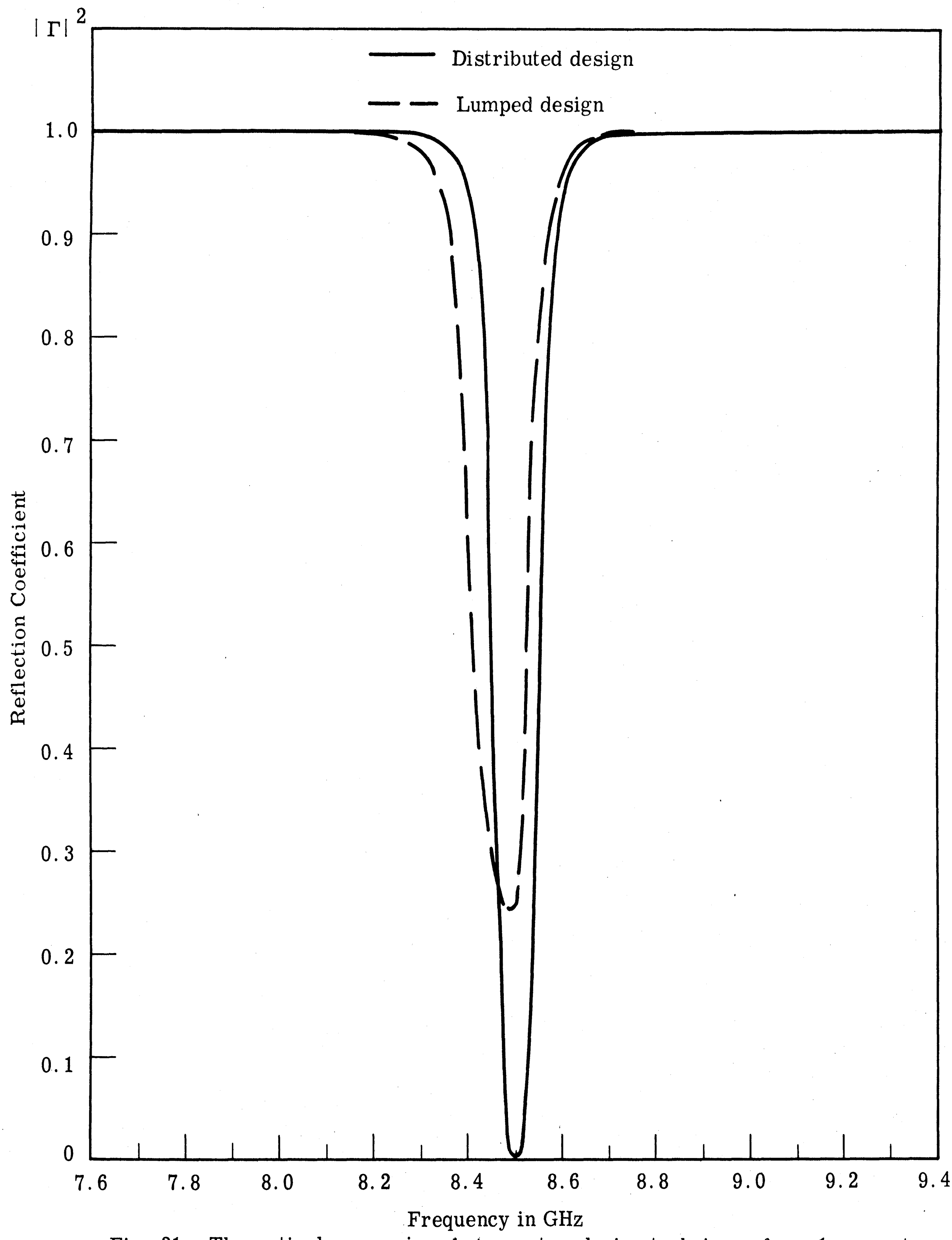

Fig. 31. Theoretical comparison between two design techniques for a 1 percent bandwidth impedance transformer operating between a 50-ohm and a 1-ohm load

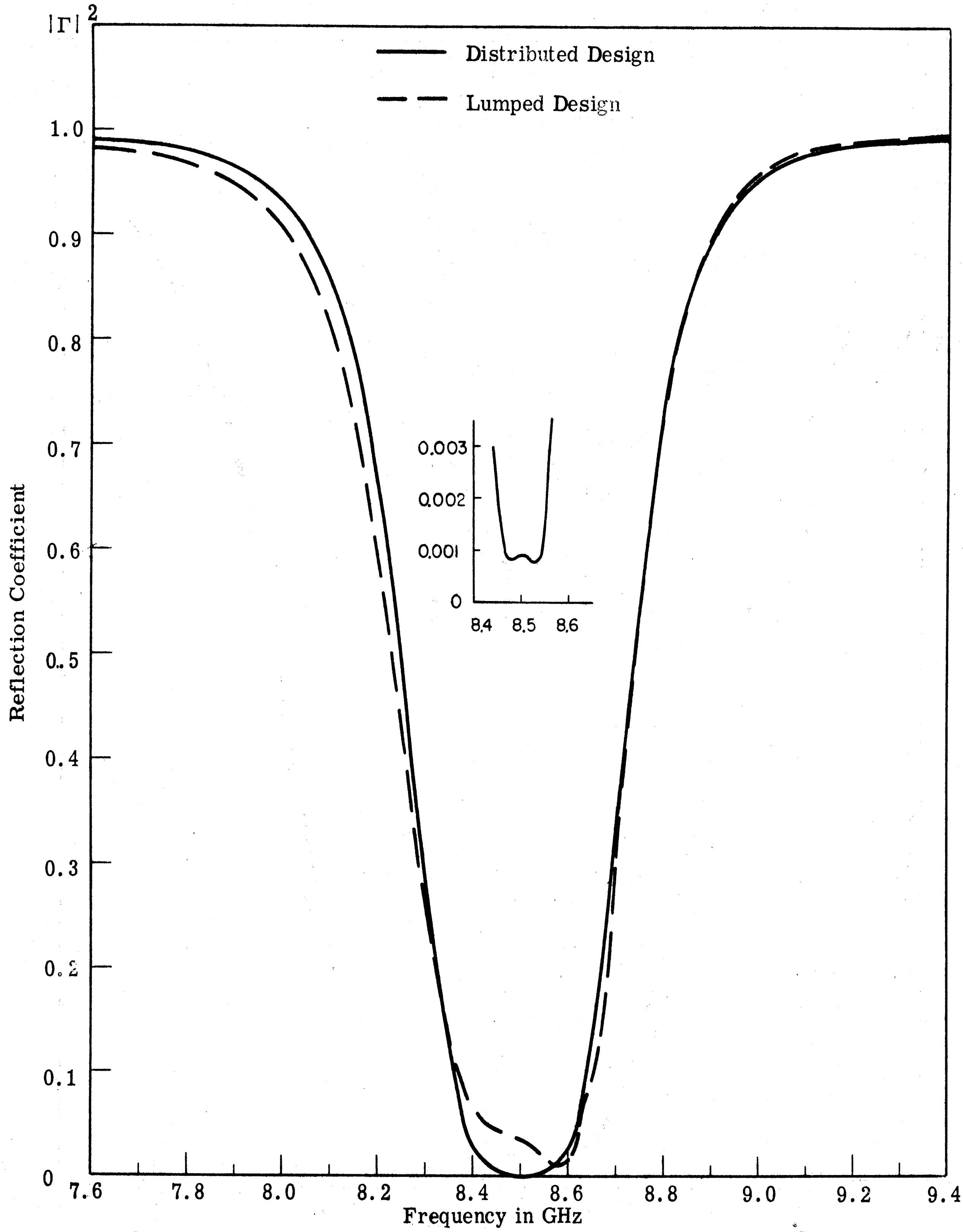

Fig. 32. Theoretical comparison between two design techniques for a 5 percent bandwidth impedance transformer operating between a 50-ohm and a 1-ohm load

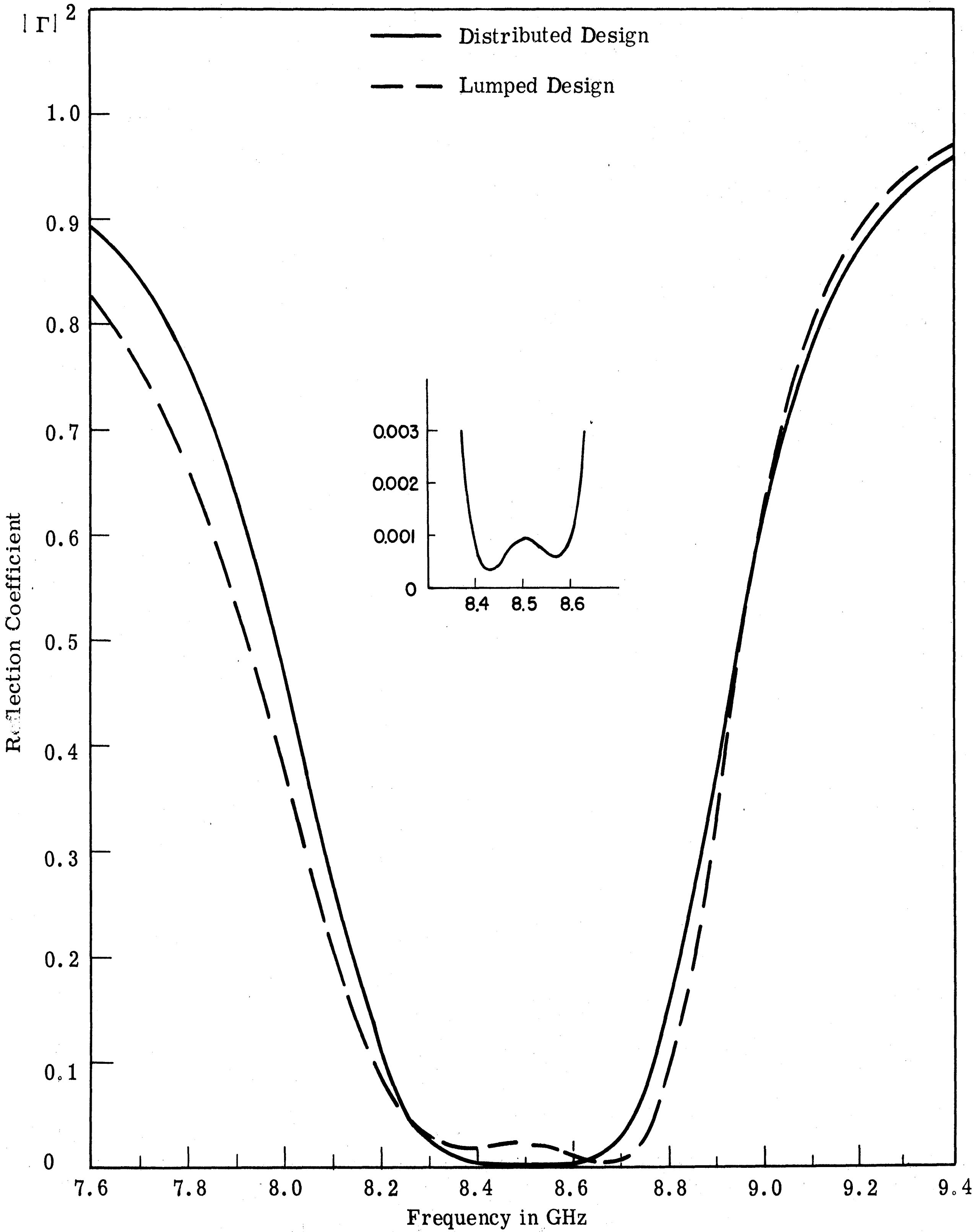

Fig. 33. Theoretical comparison between two design techniques for a 10 percent bandwidth impedance transformer operating between a 50-ohm and a 1-ohm load

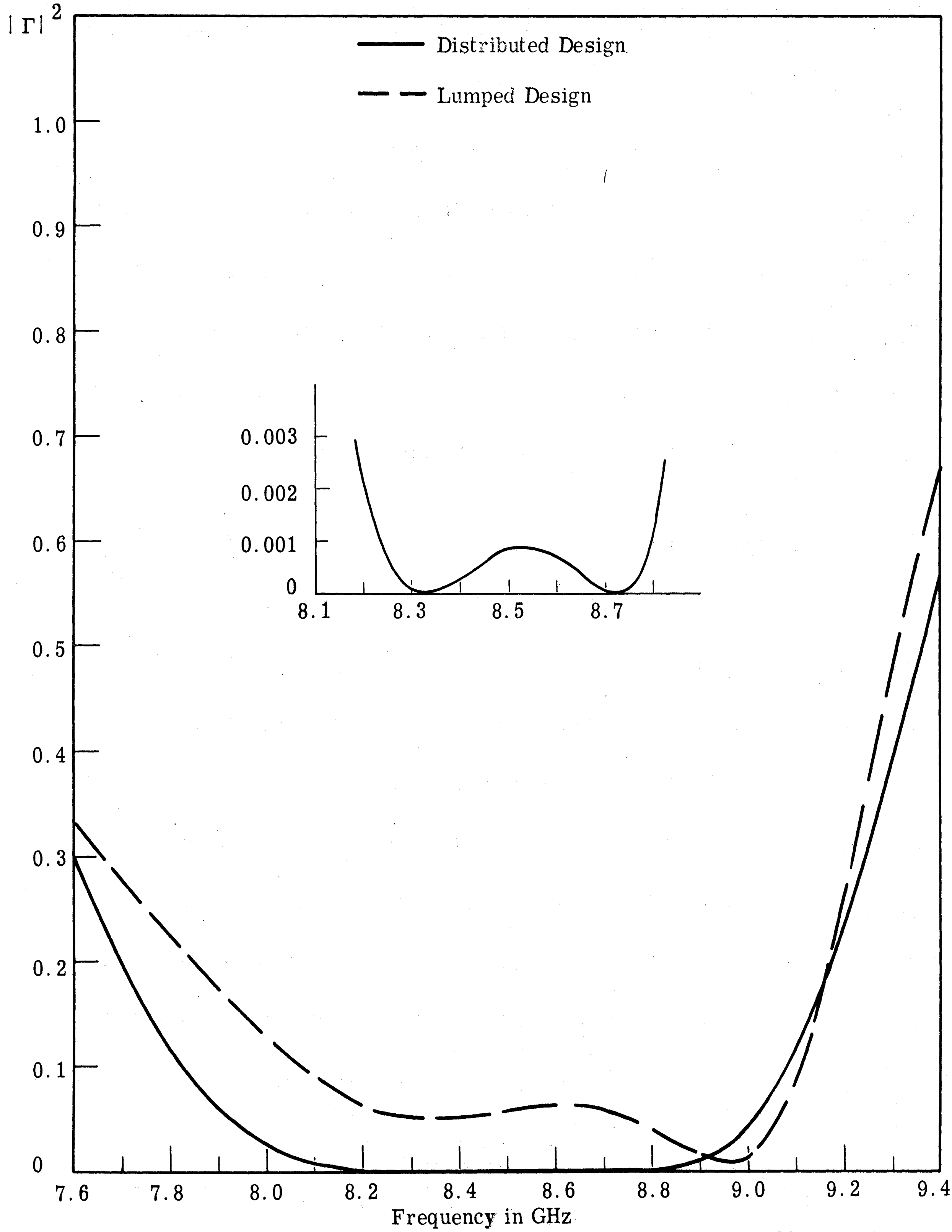

Fig. 34. Theoretical comparison between two design techniques for a 20 percent bandwidth impedance transformer operating between a 50-ohm and a 1-ohm load

transformers generally had a flatter passband and a slightly narrower bandwidth than the design goal. Table III summarizes the design data for these curves.

XIII c. Impedance Plots. The impedance of the 10 percent bandpass filter shown in Fig. 28 is plotted in Fig. 35. The impedance seen from the 1-ohm side of the transformer of Fig. 33 is plotted in Fig. 36. An ideal filter would have an impedance of 50 + j0 ohms in the passband in Fig. 35, and an ideal impedance matching network would have an impedance of 1 + j0 ohms in the passband of Fig. 36.

XIV. Experimental Work

A 50-ohm to 50-ohm bandpass filter with a 10 percent bandwidth was constructed using the distributed design technique. The same ripple and g values were used as before, and the center frequency was chosen as 8.5 GHz. The design procedure of Section XII was used to build a filter of the form shown in Fig. 37. For ease of handling the outer two disks were made thicker by using an air dielectric between the outer conductor and the disk. The center two disks had a Teflon dielectric ($\epsilon_r = 2.03$) between the two conductors to increase the capacitance and to provide mechanical support for the disks. Here the disk lengths, ℓ_i, have been shortened in accord with Eq. 42 to account for the discontinuity capacitance. The final design parameters are shown in Table IV.

Lumped or Distributed	Band-width w	Disk Diameters											
		K_1	K_2	K_3	D_1 in.	D_2 in.	D_3 in.	ℓ_1 cm	ℓ_2 cm	ℓ_3 cm	ϕ_1 rad.	ϕ_2 rad.	ϕ_3 rad.
L	1%	0.7338	0.6973	6.5221	0.554	0.554	0.502	0.3439	0.3620	0.2843	0.02935	0.02789	0.25942
D	1%	"	"	"	"	"	"	0.4183	0.4591	0.3215	0.01431	0.01100	0.17667
L	5%	1.6409	3.4864	14.5839	0.542	0.532	0.502	0.3747	0.2638	0.1184	0.06561	0.13923	0.56761
D	5%	"	"	"	"	"	"	0.4963	0.2899	0.1214	0.02006	0.10307	0.53787
L	10%	2.3206	6.9727	20.6247	0.542	0.502	0.502	0.2647	0.2653	0.0759	0.0276	0.27712	0.78246
D	10%	"	"	"	"	"	"	0.2906	0.2944	0.0771	0.06861	0.20206	0.76366
L	20%	3.2818	13.9454	26.1678	0.532	0.502	0.502	0.2804	0.1248	0.0427	0.13108	0.54399	1.05618
D	20%	"	"	"	"	"	"	0.3129	0.1282	0.0432	0.09173	0.51256	1.04568

Table III. Disk parameters for bandpass impedance transformer using three disks

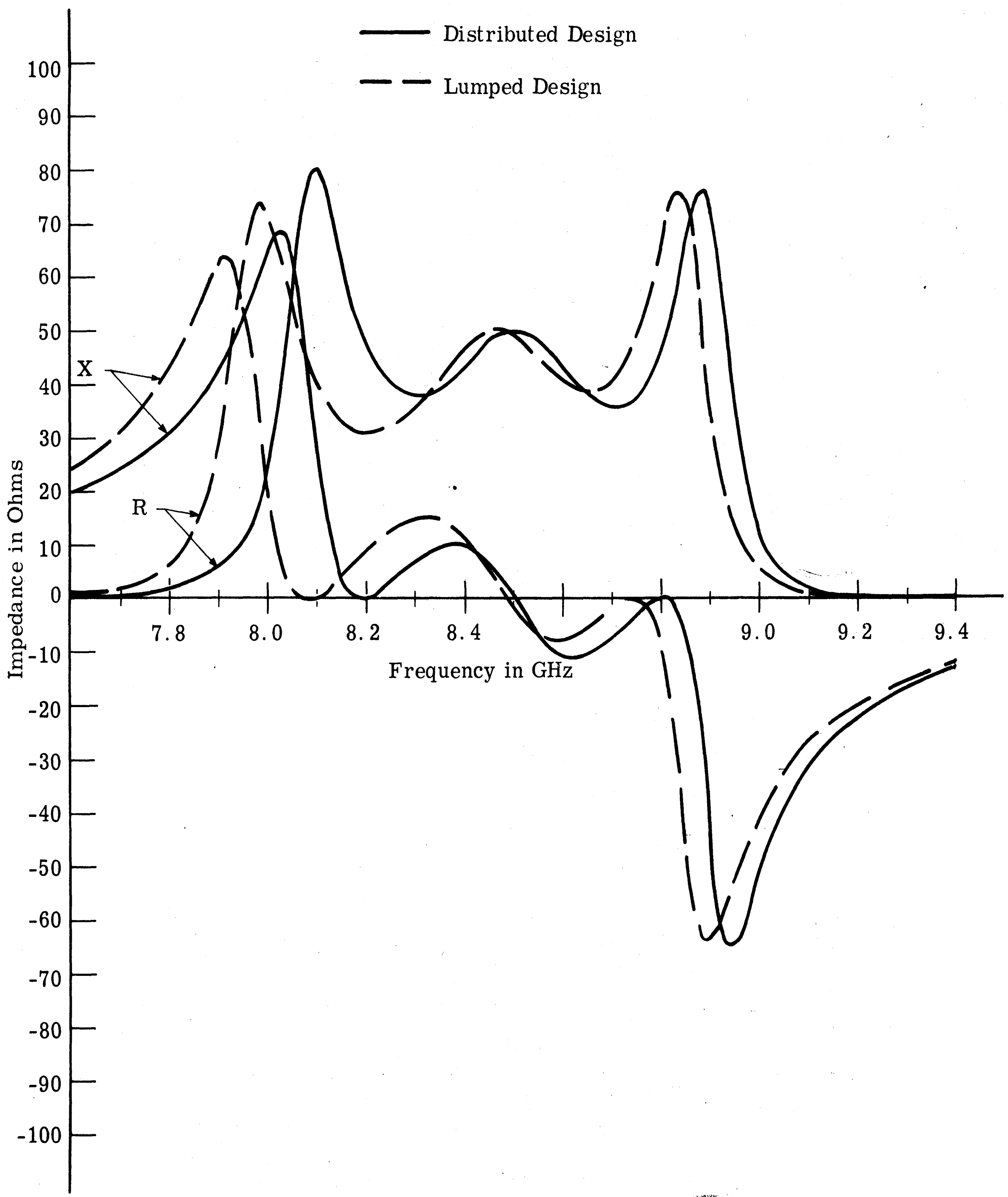

Fig. 35. Theoretical impedance of a 3-ripple, 10 percent bandwidth bandpass filter operating between two 50-ohm loads

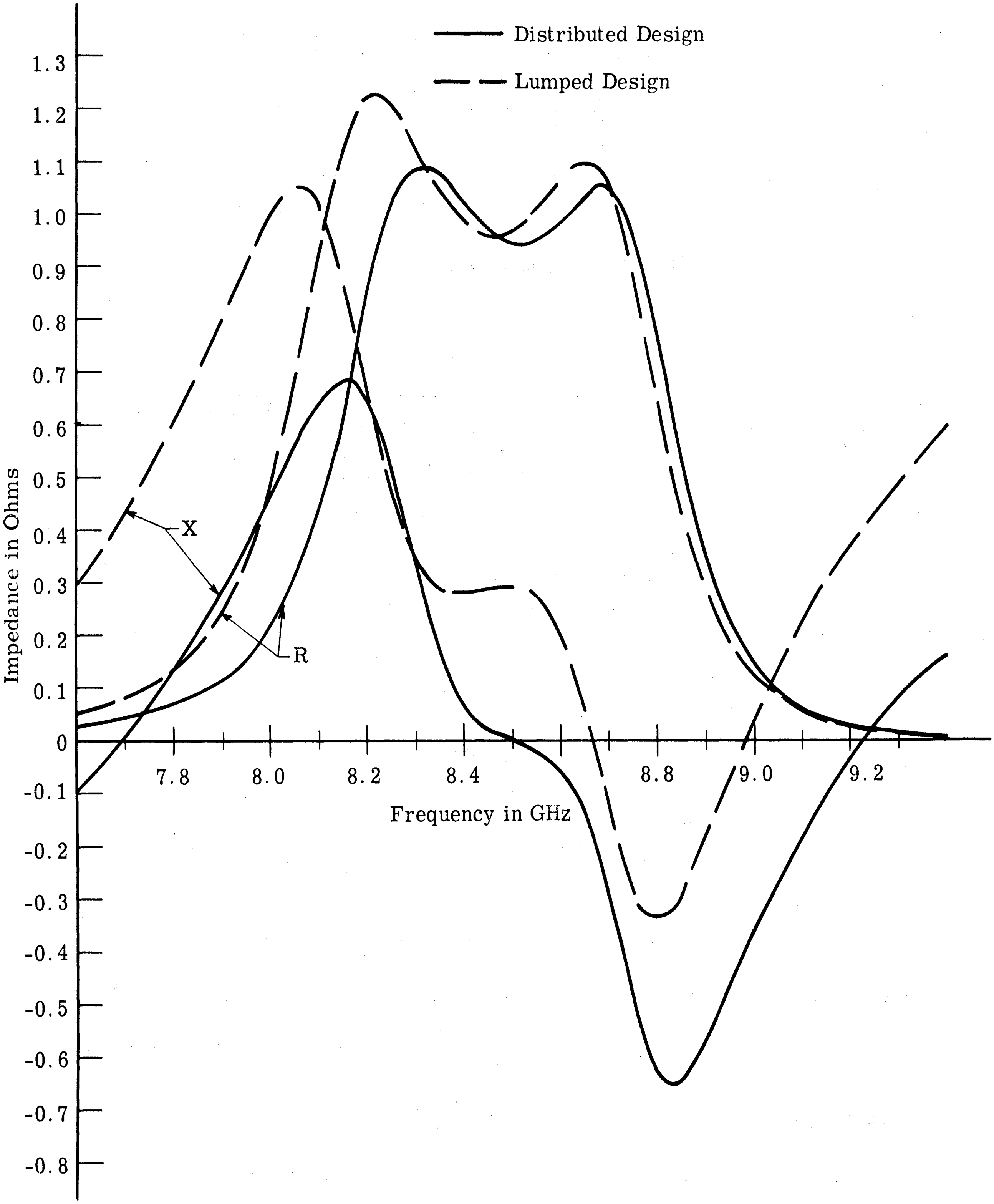

Fig. 36. Theoretical impedance of a 3-ripple, 10 percent bandwidth 50 impedance transformer as seen from the 1-ohm side

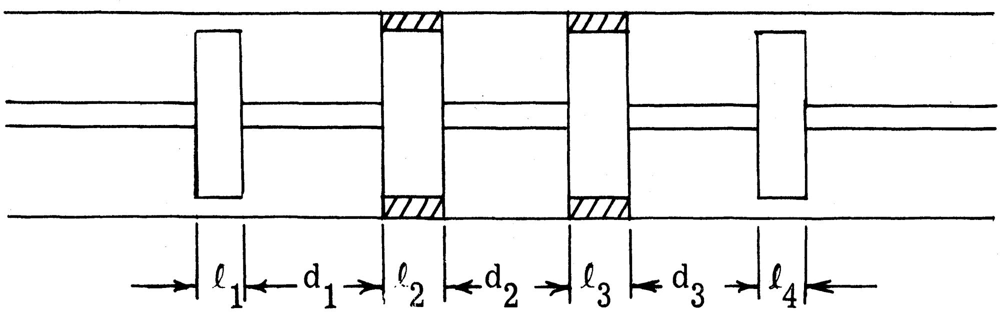

Fig. 37. Coaxial bandpass filter

K_1	$= 19.51168$
K_2	$= 7.219345$
ϕ_1	$= 0.7019$ radians
ϕ_2	$= 0.2153$ radians
All disk diameters	$= 0.502$ in.
$\ell_1 = \ell_4$	$= 0.01456$ in.
$\ell_2 = \ell_3$	$= 0.08465$ in.
$d_1 = d_3$	$= 0.79564$ in.
d_2	$= 0.74186$ in.

Table IV. Filter design parameters

The theoretical bandpass characteristics for this filter are shown in Fig. 38 and the experimental curve is shown in Fig. 39. In both cases the high frequency ripple is the larger one, the ripple in the experiment filter being slightly larger than the theoretical one. The dip in the middle of the large ripple in Fig. 39 appears to be a small resonance due to a mismatch in the line, quite possibly in a connector. The attenuation in the out of band frequencies was lower in Fig. 39 because the high VSWR was limited by losses in the system.

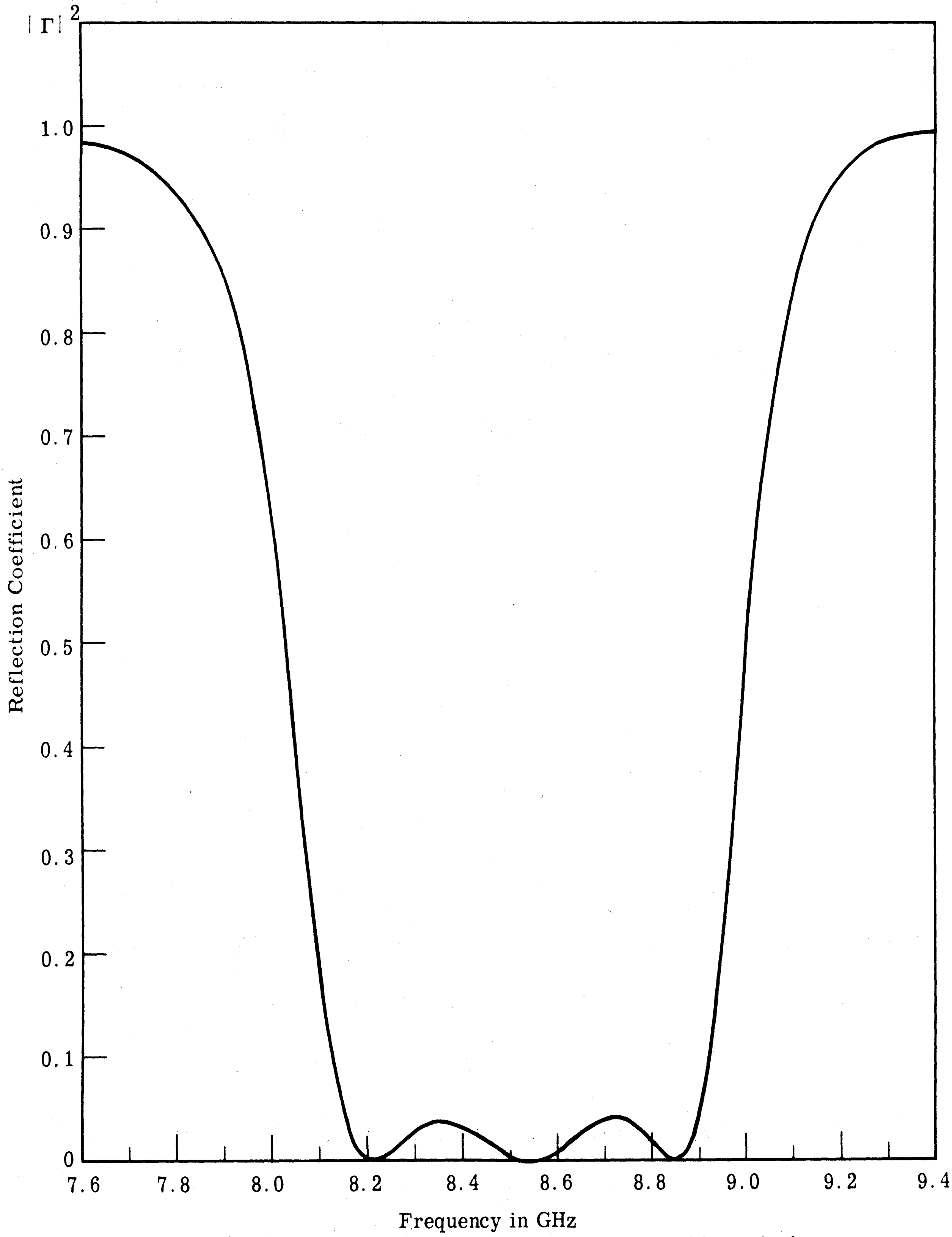

Fig. 38. Theoretical 10 percent bandiwdth bandpass filter which accounts for discontinuity capacitance

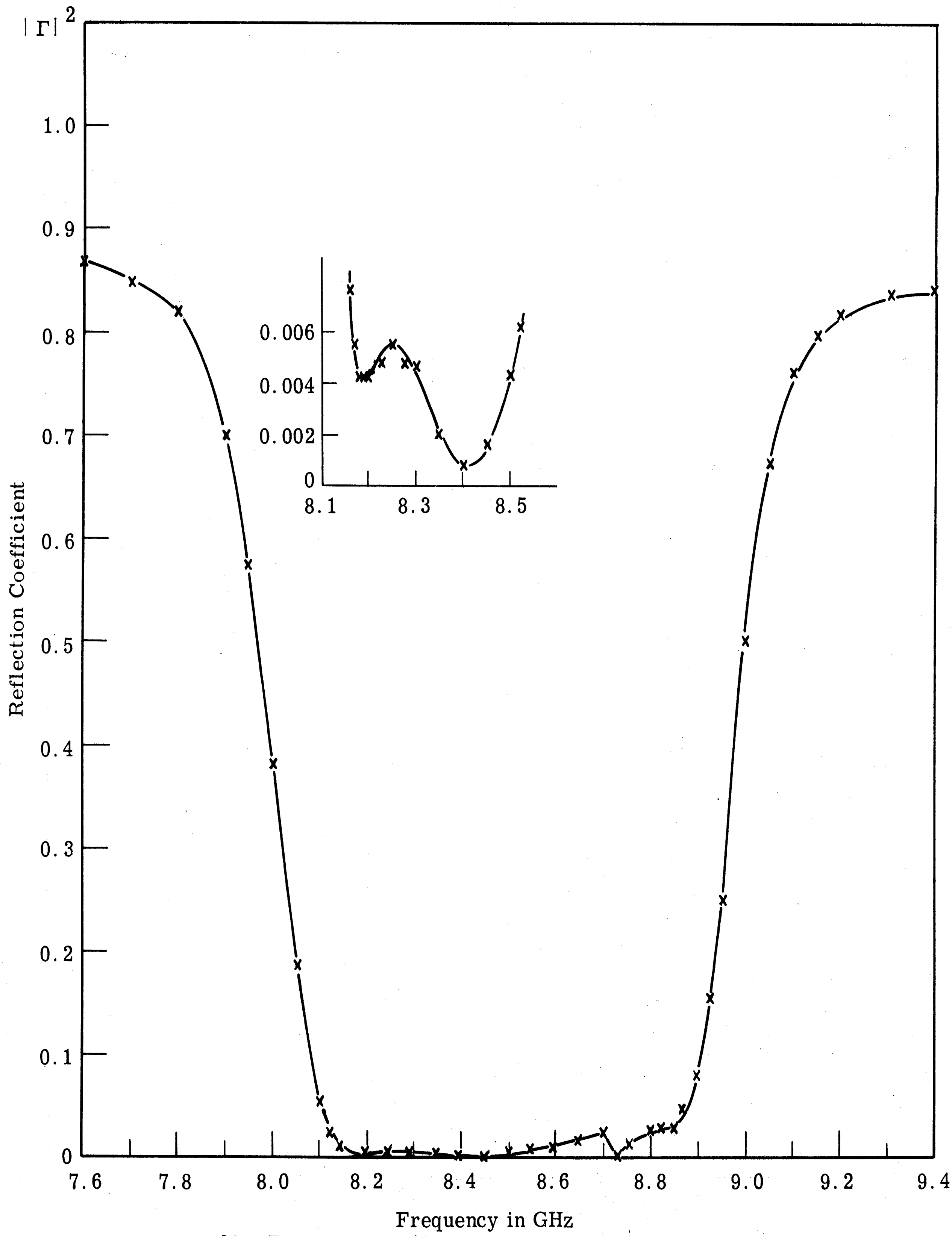

Fig. 39. Experimental 10 percent bandwidth bandpass filter

XV. Conclusions

The distributed design procedure developed here for bandpass filters and impedance transformers gives an improved overall characteristic over the lumped design procedure. Although the distributed design gives a lower ripple than the lumped design, it is still larger than the low-pass prototype design ripple. The design method itself is easy to use and is applicable over a wide range of microwave frequencies.

REFERENCES

1. S. B. Cohn, "Direct Coupled Resonator Filters," Proc. IRE 45, February 1957, pp. 187-196.

2. R. E. Collin, Foundations for Microwave Engineering, McGraw-Hill, 1966.

3. E. A. Guillemin, Synthesis of Passive Networks, John Wiley and Sons, New York, 1957.

4. G. L. Matthaei, L. Young, and E. M. T. Jones, Microwave Filters, Impedance-Matching Networks, and Coupling Structures, McGraw-Hill, New York, 1965.

5. F. F. Kuo, Network Analysis and Synthesis, John Wiley and Sons, New York, 1962.

6. P. I. Somlo, "The Computation of Coaxial Line Step Capacitances," IEEE Trans. on Microwave Theory and Techniques, MTT-15, No. 1, January 1967.

DISTRIBUTION LIST

No. of Copies	
20	National Security Agency Ft. George G. Meade, Maryland 20755
1	Technical Library Dir. of Defense Research & Engineering Rm. 3E-1039, The Pentagon Washington, D.C. 20301
1	Defense Intelligence Agency Attn: DIARD Washington, D.C. 20301
2	Director National Security Agency Attn: C31 Ft. George G. Meade, Maryland 20755
1	Naval Ships Systems Command Attn: Code 20526 (Technical Library) Main Navy Building, Rm. 1528 Washington, D.C. 20325
1	Naval Ships Systems Command Attn: Code 6179B Department of the Navy Washington, D.C. 20360
2	Director U.S. Naval Research Laboratory Attn: Code 2027 Washington, D.C. 20390
1	Commanding Officer and Director U.S. Navy Electronics Laboratory Attn: Library San Diego, California 92152

DISTRIBUTION LIST (Cont.)

No. of Copies	
1	Commander U.S. Naval Ordnance Laboratory Attn: Technical Library White Oak, Silver Spring, Maryland 20910
1	AFSC STLO (RTSND) Naval Air Development Center Johnsville, Warminster, Pa. 18974
1	Dir. Marine Corps Landing Force Dev Ctr Attn: C-E Division Marine Corps Schools Quantico, Virginia 22134
1	Commandant of the Marine Corps (Code AO2F) Headquarters, U.S. Marine Corps Washington, D.C. 20380
1	Rome Air Development Center (EMTLD) Attn: Documents Library Griffiss Air Force Base New York 13440
1	U.S. Army Security Agency Test and Evaluation Center Fort Huachuca, Arizona 85613 Code IAOVT
2	Electronic Systems Division (ESTI) L.G. Hanscom Field Bedford, Massachusetts 01730
1	U.S. Air Force Security Service Attn: TSG, VICE Attn: ESD San Antonio, Texas 78241

DISTRIBUTION LIST (Cont.)

No. of Copies	
1	Air Proving Ground Ctr (PGBPS-12) Attn: PGAPI Eglin Air Force Base, Florida 32542
1	Headquarters, AFSC Attn: SCTSE Bolling AFB, D.C. 20332
1	Air University Library (3T) Maxwell Air Force Base, Alabama 36112
1	HQ, USAF Tactical Air Recon Ctr (TAC) Department of the Air Force Shaw Air Force Base, South Carolina 29152
2	Chief of Research and Development Department of the Army Washington, D.C. 20315
2	Commanding General U.S. Army Materiel Command Attn: R&D Directorate Washington, D.C. 20315
3	Redstone Scientific Information Center Attn: Chief, Document Section U.S. Army Missile Command Redstone Arsenal, Alabama 35809
1	Headquarters U.S. Army Weapons Command Attn: AMSWE-RDR Rock Island, Illinois 61201
1	Commanding Officer 52D USASASOC Fort Huachuca, Arizona 85613

DISTRIBUTION LIST (Cont.)

No. of Copies	
2	Commanding Officer Aberdeen Proving Ground Attn: Technical Library, Bldg. 313 Aberdeen Proving Ground, Maryland 21005
2	Headquarters U.S. Army Materiel Command Attn: AMCMA-RM/3 Washington, D.C. 20315
1	Commanding General U.S. Army Combat Developments Command Attn: CDCMR-E Fort Belvoir, Virginia 22060
3	Commanding Officer U.S. Army Combat Developments Command Communications-Electronics Agency Fort Monmouth, New Jersey 07703
1	Commander U.S. Army Research Office (DURHAM) Box CM-DUKE Station Durham, North Carolina 27706
1	Commanding Officer U.S. Army Sec Agcy Combat Dev Actv Arlington Hall Station Arlington, Virginia 22212
1	U.S. Army Security Agency Attn: OACofS, DEV Arlington Hall Station Arlington, Virginia 22212

DISTRIBUTION LIST (Cont.)

No. of Copies	
1	U.S. Army Security Agcy Processing Ctr Attn: IAVAPC-R&D Vint Hill Farms Station Warrenton, Virginia 22186
1	Technical Support Directorate Attn: Technical Library Bldg. 3330, Edgewood Arsenal Maryland 21010
2	Commanding Officer U.S. Army Nuclear Defense Laboratory Attn: Library Edgewood Arsenal, Maryland 21010
1	Harry Diamond Laboratories Attn: Library Connecticut Avenue and Van Ness Street Washington, D.C. 20438
1	Commandant U.S. Army Air Defense School Attn: C&S Dept. MSL SCI DIV Fort Bliss, Texas 79916
1	Commanding General U.S. Army Electronic Proving Ground Attn: Technical Information Center Fort Huachuca, Arizona 85613
1	Asst. Secretary of the Army (R&D) Department of the Army Attn: Deputy Asst. for Army (R&D) Washington, D.C. 20315
1	Commanding Officer U.S. Army Limited War Laboratory Aberdeen Proving Ground, Md. 21005

DISTRIBUTION LIST (Cont.)

No. of Copies	
1	Ch, Special Techniques Division Unconventional Warfare Department U.S. Army Special Warfare School Fort Bragg, North Carolina 28307
1	Commanding Officer U.S. Foreign Science & Tech Ctr Attn: AMXST-RD-R, Munitions Bldg Washington, D.C. 20315
1	Office, AC of S for Intelligence Department of the Army Attn: ACSI-DSRS Washington, D.C. 20310
1	Chief, Mountain View Office EW Lab USAECOM Attn: AMSEL-WL-RU P.O. Box 205 Mountain View, California 94042
1	Chief, Intelligence Materiel Dev Office Electronic Warfare Lab., USAECOM Fort Holabird, Maryland 21219
1	Chief Missile Electronic Warfare Tech Area EW Lab, USA Electronics Command White Sands Missile Range, N.M. 88002
1	Headquarters U.S. Army Combat Developments Command Attn: CDCLN-EL Fort Belvoir, Virginia 22060
1	USAECOM Liaison Officer MIT, Bldg. 26, Rm. 131 77 Massachusetts Avenue Cambridge, Mass. 02139

DISTRIBUTION LIST (Cont.)

No. of Copies	
1	USAECOM Liaison Officer Aeronautical Systems Division Attn: ASDL-9 Wright-Patterson AF Base, Ohio 45433
1	USAECOM Liaison Office U.S. Army Electronic Proving Ground Fort Huachuca, Arizona 85613
20	Commanding General U.S. Army Electronics Command Fort Monmouth, New Jersey 07703 Attn: 1 AMSEL-IM 1 AMSEL-EW 1 AMSEL-PP 1 AMSEL-IO-T 1 AMSEL-RD-MAT 1 AMSEL-RD-LNA 1 AMSEL-RD-LNJ 1 AMSEL-XL-D 1 AMSEL-NL-D 1 AMSEL-VL-D 1 AMSEL-KL-D 3 AMSEL-HL-CT-D 1 AMSEL-BL-D 3 AMSEL-WL 1 AMSEL-WL (ofc. of records) 1 AMSEL-SC
1	Dr. T. W. Butler, Jr., Director Cooley Electronics Laboratory The University of Michigan Ann Arbor, Michigan 48105
22	Cooley Electronics Laboratory The University of Michigan Ann Arbor, Michigan 48105

UNCLASSIFIED
Security Classification

DOCUMENT CONTROL DATA - R&D

(Security classification of title, body of abstract and indexing annotation must be entered when the overall report is classified)

1. ORIGINATING ACTIVITY (Corporate author) Cooley Electronics Laboratory The University of Michigan Ann Arbor, Michigan	2a. REPORT SECURITY CLASSIFICATION UNCLASSIFIED 2b. GROUP

3. REPORT TITLE

COAXIAL MICROWAVE BANDPASS FILTERS

4. DESCRIPTIVE NOTES (Type of report and inclusive dates)

C. E. L. Technical Memorandum No. 100 May 1969

5. AUTHOR(S) (Last name, first name, initial)

Davis, W. A.

6. REPORT DATE	7a. TOTAL NO. OF PAGES	7b. NO. OF REFS
May 1969	75	6

8a. CONTRACT OR GRANT NO. DAAB 07-68-C-0138 b. PROJECT NO. 1 HO 21101 A04 01 02 c. d.	9a. ORIGINATOR'S REPORT NUMBER(S) 1482-5 TM 100 9b. OTHER REPORT NO(S) (Any other numbers that may be assigned this report) ECOM-0138-5

10. AVAILABILITY/LIMITATION NOTICES This document is subject to special controls and each transmittal to foreign governments or foreign nationals may be made only with prior approval of CG, U.S. Army Electronics Command, Ft. Monmouth, N.J. Attn: AMSEL-WL-S.

11. SUPPLEMENTARY NOTES	12. SPONSORING MILITARY ACTIVITY U.S. Army Electronics Command Fort Monmouth, New Jersey 07703 Attn: AMSEL-WL-S

13. ABSTRACT

A review of lumped-element filter synthesis techniques using the power loss ratio is presented. This leads to filter synthesis based on impedance inverters for which S. B. Cohn (Ref. 1) has given an approximate microwave realization. Here an improved method is presented which considers the distributive property of the impedance inverter. Several theoretical curves are shown comparing the two methods. Finally results from an experimental model are shown.

DD FORM 1 JAN 64 1473

UNCLASSIFIED
Security Classification

UNCLASSIFIED
Security Classification

14. KEY WORDS	LINK A		LINK B		LINK C	
	ROLE	WT	ROLE	WT	ROLE	WT
Microwaves Bandpass Filters Impedance Inverter Matching Network						

INSTRUCTIONS

1. ORIGINATING ACTIVITY: Enter the name and address of the contractor, subcontractor, grantee, Department of Defense activity or other organization *(corporate author)* issuing the report.

2a. REPORT SECURITY CLASSIFICATION: Enter the overall security classification of the report. Indicate whether "Restricted Data" is included. Marking is to be in accordance with appropriate security regulations.

2b. GROUP: Automatic downgrading is specified in DoD Directive 5200.10 and Armed Forces Industrial Manual. Enter the group number. Also, when applicable, show that optional markings have been used for Group 3 and Group 4 as authorized.

3. REPORT TITLE: Enter the complete report title in all capital letters. Titles in all cases should be unclassified. If a meaningful title cannot be selected without classification, show title classification in all capitals in parenthesis immediately following the title.

4. DESCRIPTIVE NOTES: If appropriate, enter the type of report, e.g., interim, progress, summary, annual, or final. Give the inclusive dates when a specific reporting period is covered.

5. AUTHOR(S): Enter the name(s) of author(s) as shown on or in the report. Enter last name, first name, middle initial. If military, show rank and branch of service. The name of the principal author is an absolute minimum requirement.

6. REPORT DATE: Enter the date of the report as day, month, year; or month, year. If more than one date appears on the report, use date of publication.

7a. TOTAL NUMBER OF PAGES: The total page count should follow normal pagination procedures, i.e., enter the number of pages containing information.

7b. NUMBER OF REFERENCES: Enter the total number of references cited in the report.

8a. CONTRACT OR GRANT NUMBER: If appropriate, enter the applicable number of the contract or grant under which the report was written.

8b, 8c, & 8d. PROJECT NUMBER: Enter the appropriate military department identification, such as project number, subproject number, system numbers, task number, etc.

9a. ORIGINATOR'S REPORT NUMBER(S): Enter the official report number by which the document will be identified and controlled by the originating activity. This number must be unique to this report.

9b. OTHER REPORT NUMBER(S): If the report has been assigned any other report numbers *(either by the originator or by the sponsor)*, also enter this number(s).

10. AVAILABILITY/LIMITATION NOTICES: Enter any limitations on further dissemination of the report, other than those imposed by security classification, using standard statements such as:

(1) "Qualified requesters may obtain copies of this report from DDC."

(2) "Foreign announcement and dissemination of this report by DDC is not authorized."

(3) "U. S. Government agencies may obtain copies of this report directly from DDC. Other qualified DDC users shall request through ________________."

(4) "U. S. military agencies may obtain copies of this report directly from DDC. Other qualified users shall request through ________________."

(5) "All distribution of this report is controlled. Qualified DDC users shall request through ________________."

If the report has been furnished to the Office of Technical Services, Department of Commerce, for sale to the public, indicate this fact and enter the price, if known.

11. SUPPLEMENTARY NOTES: Use for additional explanatory notes.

12. SPONSORING MILITARY ACTIVITY: Enter the name of the departmental project office or laboratory sponsoring *(paying for)* the research and development. Include address.

13. ABSTRACT: Enter an abstract giving a brief and factual summary of the document indicative of the report, even though it may also appear elsewhere in the body of the technical report. If additional space is required, a continuation sheet shall be attached.

It is highly desirable that the abstract of classified reports be unclassified. Each paragraph of the abstract shall end with an indication of the military security classification of the information in the paragraph, represented as *(TS)*, *(S)*, *(C)*, or *(U)*.

There is no limitation on the length of the abstract. However, the suggested length is from 150 to 225 words.

14. KEY WORDS: Key words are technically meaningful terms or short phrases that characterize a report and may be used as index entries for cataloging the report. Key words must be selected so that no security classification is required. Identifiers, such as equipment model designation, trade name, military project code name, geographic location, may be used as key words but will be followed by an indication of technical context. The assignment of links, rules, and weights is optional.

UNCLASSIFIED